

Cite this: *Catal. Sci. Technol.*, 2022,  
12, 4709

# Enantioselective Michael addition of aldehydes to maleimides catalysed by surface-adsorbed natural amino acids†‡

Viktória Kozma<sup>a</sup> and György Szöllösi \*<sup>b</sup>

Asymmetric Michael addition of carbonyl compounds to *N*-substituted maleimides is an important method for obtaining optically pure succinimides, which are important chiral fine chemical intermediates. Environmentally friendly and sustainable procedures require the use of a heterogeneous, recyclable catalyst obtained from natural chirality sources and cheap auxiliaries. Here we report the application of *in situ* formed chiral inorganic–organic hybrid catalysts using amino acids such as *L*-phenylalanine and clay minerals or alumina, which were highly active and provided excellent enantioselectivities, up to 99%, in the addition of aldehydes to a large variety of *N*-substituted maleimides. Examinations indicated the occurrence of the asymmetric reaction on the surface of the recyclable solid hybrid materials. The catalytic materials were examined by thermogravimetry, XRD, FT-IR and Raman spectroscopy, SEM and adsorption experiments. Results of these methods showed that the amino acid is deposited as surface crystallites or intercalated in the layered cation exchangers, which both function as a supply of the chirality source, whereas the reactions are catalysed by the chiral compounds adsorbed on the surface. This catalytic system was used to conveniently prepare chiral succinimides at the gram scale, easily purified by crystallization. Accordingly, these chiral hybrid materials are convenient heterogeneous catalysts for obtaining valuable compounds in high optical purities using natural chirality sources, inorganic solids and ethyl acetate, a green organic solvent.

Received 21st March 2022,  
Accepted 30th May 2022

DOI: 10.1039/d2cy00545j

rsc.li/catalysis

## Introduction

The development of novel procedures for the preparation of optically pure organic compounds is among the important goals of modern organic chemistry, since the chiral products obtained have wide application areas, such as intermediates for the agrochemical, food, fragrance and pharmaceutical industries.<sup>1–4</sup> Presently, besides economic considerations the sustainability and environmental impact of the new processes must be taken into account. This motivated the application of asymmetric catalytic processes, which allow decreased amounts of chirality sources used in enantioselective reactions.<sup>5–7</sup> During the last few decades, besides chiral metal complexes, optically pure organic compounds, so-called organocatalysts, were also found highly efficient in catalysing

a large variety of stereoselective reactions.<sup>8–11</sup> Among these are various C–C coupling reactions, such as organocatalyzed asymmetric conjugate additions, leading to optically pure products with increased complexities.<sup>12,13</sup>

Chiral succinimides are structural units found in several natural products and drug candidates.<sup>14–16</sup> These chiral motifs are conveniently accessed by asymmetric conjugate additions of various nucleophiles to maleimides.<sup>17</sup> Accordingly, the enantioselective organocatalytic Michael additions to maleimides have been extensively investigated in the last fifteen years. Several types of catalysts have been developed for these purposes, *i.e.* cinchona alkaloids and derivatives thereof,<sup>18–21</sup> chiral pyrrolidine derivatives,<sup>22,23</sup> *C*<sub>2</sub>-symmetric 1,2-diamine derivatives,<sup>24–37</sup> amino acids and oligopeptides,<sup>38–43</sup> and others.<sup>44–46</sup> The chiral bifunctional organocatalysts bearing primary amine groups were employed mostly in the asymmetric addition of aldehydes and/or ketones to maleimides. The most efficient amino acid derivatives used for these purposes were the <sup>t</sup>Bu-ether of *L*-threonine, mono <sup>t</sup>Bu-ester of *L*-aspartic acid and  $\beta$ -phenylalanine. These were used either in combination with basic additives ensuring the *in situ* formation of the corresponding salts or as inorganic salts.<sup>38,39,43</sup> Natural, unfunctionalized  $\alpha$ -amino acids were less examined due to

<sup>a</sup> Department of Organic Chemistry, University of Szeged, 6720 SzegedDóm tér 8, Hungary<sup>b</sup> SZTE-ELKH Stereochemistry Research Group, University of Szeged, 6720 SzegedEötvös utca 6, Hungary. E-mail: szollosi@chem.u-szeged.hu

† Dedicated to the memory of Prof. István Pálinkó.

‡ Electronic supplementary information (ESI) available: Additional optimization and solid hybrid characterization data, spectra and chromatograms of the prepared organic compounds are provided. See DOI: <https://doi.org/10.1039/d2cy00545j>

their slightly poorer performances compared to the above derivatives, although, *L*-isoleucine (*L*-Ile) or *L*-phenylalanine (*L*-Phe) was also found efficient in the addition of aldehydes to maleimides.<sup>38,39</sup>

Albeit the above asymmetric catalytic methods allowed the preparation of chiral succinimides in high optical purities, further studies were necessary to develop more environmentally friendly and sustainable methods. A major step in reaching these goals is the application of heterogeneous catalysts, which may allow simple separation and recycling of the catalysts. Up to now large varieties of chiral heterogeneous catalysts have been developed.<sup>47–51</sup> Among these were few materials designed to catalyse the enantioselective addition of carbonyl compounds to maleimides as well. However, most of the latter were obtained by covalent bonding of the optically pure organocatalysts to insoluble supports, which needed several, sometimes synthetically demanding, preparation steps.<sup>52–60</sup> Only in few procedures was covalent immobilization of the catalytic materials avoided. Thus, optically pure hyperbranched polymers worked in a synergistic way with quinine to afford succinimides with moderate enantioselectivities.<sup>61</sup> Very recently, Juaristi and co-workers intercalated amino acids (*L*-Phe, *L*-tryptophane (*L*-Trp) and *D*-Phe) and two  $\alpha,\beta$ -dipeptides in layered double hydroxides by anion-exchange and used these hybrid solids in the addition of  $\alpha$ -branched aldehydes to maleimides. High yields and enantioselectivities were reached in reactions, which were suggested to occur in the interlayer space of the chiral solids.<sup>62</sup>

A simpler method of getting chiral solids active in asymmetric catalytic reactions is the adsorption of organocatalysts on appropriate supports. Early attempts used catalytically active oxide surfaces modified by *in situ* adsorbed chiral organic compounds.<sup>63–65</sup> Latter, in some reactions significantly improved activities and/or enantioselectivities or even change of the enantiodifferentiation sense were observed by applying organocatalysts adsorbed on solid inorganic oxide surfaces compared to the corresponding homogeneous chiral catalysts.<sup>66–69</sup> Recently, a surface-improved asymmetric reaction was developed using *in situ* adsorbed *L*-proline (*L*-Pro) over LAPONITE® (Lap),<sup>70</sup> a synthetic layered magnesium silicate cation-exchanger clay.<sup>71</sup> The Michael addition of aldehydes to  $\beta$ -nitrostyrene occurred with exceptionally increased enantioselectivities compared to the use of *L*-Pro. Detailed studies indicated that the reaction takes place on the surface of the hybrid material; moreover, the performance of the primary amino acids (*L*-valine (*L*-Val), *L*-Phe, *L*-Trp) was also improved in the presence of Lap, which interestingly, provided the opposite enantiomer in excess compared to *L*-Pro. Although in the above reaction Lap proved to afford the best enantioselectivities, other materials, such as bentonite (Ben), montmorillonite (Mon) or  $\gamma$ -Al<sub>2</sub>O<sub>3</sub> also led to highly improved results, whereas a layered double hydroxide was slightly less effective.<sup>70</sup>

Based on the above surface-improved reaction we attempted to develop a heterogeneous asymmetric catalytic

system for the addition of carbonyl compounds to maleimides using natural amino acids *in situ* adsorbed on inorganic oxide surfaces. We started our studies encouraged by the excellent results obtained in these reactions using amino acid salts,<sup>38,39,43</sup> and our expectations were strengthened by a very recent report on using *L*-Phe intercalated in layered double hydroxides published following the start of our investigations.<sup>62</sup>

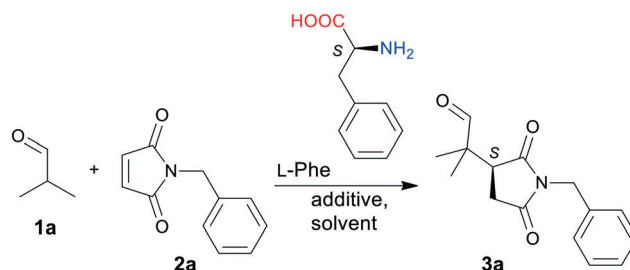
## Results and discussion

### Asymmetric Michael addition of isobutyraldehyde (1a) to *N*-benzylmaleimide (2a)

We selected the reaction of isobutyraldehyde (**1a**) and *N*-benzylmaleimide (**2a**) catalysed by *L*-Phe (Scheme 1) as a test reaction to attempt the use of a natural amino acid as a catalyst in the presence of an inorganic oxide additive. The initial reaction conditions (*i.e.* CHCl<sub>3</sub> solvent and Lap as the solid additive) were selected based on our previous experiences.<sup>70</sup> Without an additive low **2a** conversion (Conv) was reached with *L*-Phe, whereas in the presence of Lap both the Conv and the enantioselectivity (enantiomeric excess, ee) increased, reaching 96% ee (Table 1, entries 1 and 2). Due to the environmental and health problems associated with the use of chlorinated solvents,<sup>72</sup> we aimed at replacing CHCl<sub>3</sub> with a less harmful solvent. Thus, we examined the effect of the solvent nature in the presence of Lap (Table 1).

Satisfyingly, high ees were obtained in various aprotic solvents accompanied by high Convs. Under the conditions applied full Convs of **2a** and 96–97% ees were obtained in ethers, ethyl acetate (EtOAc), CH<sub>3</sub>CN and acetone. Although acetone may also react as a nucleophile with **2a**, this adduct was not detected. In protic solvents, such as alcohols the ee gradually decreased with increasing acidity (hydrogen-bond donor strength) of the –OH group. Based on these results we chose two polar aprotic solvents, *i.e.* diisopropyl ether (<sup>t</sup>Pr<sub>2</sub>O) and EtOAc to carry out further optimization experiments. The latter is among the recommended solvents in the pharmaceutical industry, which may be obtained from renewable sources.<sup>72</sup> Selected results obtained by applying various inorganic additives are summarized in Table 2.

Besides Lap another two materials afforded complete Conv of **2a** in both solvents. These are bentonite H (Ben), a



**Scheme 1** Asymmetric Michael addition of isobutyraldehyde (**1a**) to *N*-benzylmaleimide (**2a**) catalysed by *L*-phenylalanine (*L*-Phe).



**Table 1** Solvent effect in the Michael addition of **1a** to **2a** catalysed by L-Phe in the presence of Lap<sup>a</sup>

Entry	Solvent	Conv <sup>b</sup> (%)	ee <sup>c</sup> (%)
1 <sup>d</sup>	CHCl <sub>3</sub>	5	56
2	CHCl <sub>3</sub>	92	96
3	CH <sub>2</sub> Cl <sub>2</sub>	79	96
4	ClCH <sub>2</sub> CH <sub>2</sub> Cl	89	96
5	Et <sub>2</sub> O	>99	97
6	<sup>i</sup> Pr <sub>2</sub> O	>99	97
7	<sup>t</sup> BuOMe	>99	96
8	EtOAc	>99	97
9	CH <sub>3</sub> CN	>99	97
10	Tetrahydrofuran	91	95
11	(MeO) <sub>2</sub> CO	87	96
12	Acetone	>99	96
13	Toluene	98	96
14	<sup>i</sup> PrOH	>99	94
15	EtOH	>99	82
16	MeOH	>99	50

<sup>a</sup> Reaction conditions: 0.03 mmol L-Phe, 1.2 mmol **1a**, 0.3 mmol **2a**, 100 mg Lap, 1 cm<sup>3</sup> solvent, room temperature (rt), 24 h. <sup>b</sup> Conversion (Conv) determined by gas chromatography (GC). <sup>c</sup> Enantiomeric excess (ee) obtained by GC, *S* excess enantiomer, based on our previous studies.<sup>36,59</sup> <sup>d</sup> Reaction without addition of Lap, 72 h.

layered cation-exchanger clay (mostly montmorillonite) purified from native, colloidal aluminum silicate,<sup>73–75</sup> and alumina (Al<sub>2</sub>O<sub>3</sub>, neutral, pH 6.5–7.5, see the Experimental section). With these the ee increased to 98% (entries 3, 8). Similarly, high ee values (96–98%) were obtained using Na-montmorillonite (Mon), Ba(OH)<sub>2</sub>, and anion-exchanger layered double hydroxides: hydrotalcite (Htc) and LDH MG50 (entries 4–7).<sup>75</sup> However, these afforded lower Convs, except Ba(OH)<sub>2</sub>, which gave a decreased value only in EtOAc. Applying acidic solids, such as SiO<sub>2</sub>, acid treated Mon (K-10) or SiO<sub>2</sub>-supported Nafion™ H (SAC-13), led to a decrease in both the Conv and ee, especially the latter two strongly acidic materials. Thus, basic and neutral solids are appropriate additives, irrespective of their layered structure and ion-exchange properties. However, the rate of the Michael

**Table 2** Effect of the oxide additive on the enantioselective Michael addition of **1a** to **2a** catalysed by L-Phe<sup>a</sup>

Entry	Additive	Conv <sup>b</sup> (%)	ee <sup>b</sup> (%)
1	—	3; 6 <sup>c</sup>	28; 34 <sup>c</sup>
2	Lap	>99; >99 <sup>c</sup>	97; 97 <sup>c</sup>
3	Ben	>99; >99 <sup>c</sup>	98; 98 <sup>c</sup>
4	Mon	83	97
5	Htc	45	96
6	LDH MG50	66	97
7	Ba(OH) <sub>2</sub>	>99; 85 <sup>c</sup>	98; 98 <sup>c</sup>
8	Al <sub>2</sub> O <sub>3</sub>	>99; >99 <sup>c</sup>	98; 98 <sup>c</sup>
9	SiO <sub>2</sub>	67	94
10	K-10	11	67
11	SAC-13	5	41

<sup>a</sup> Reaction conditions: 0.03 mmol L-Phe, 1.2 mmol **1a**, 0.3 mmol **2a**, 100 mg additive, 1 cm<sup>3</sup> <sup>i</sup>Pr<sub>2</sub>O solvent, rt, 24 h. <sup>b</sup> Conversion (Conv) and enantiomeric excess (ee) determined by GC, *S* excess enantiomer. <sup>c</sup> Result obtained in 1 cm<sup>3</sup> EtOAc.

addition was sensitive to the surface properties of the additive, possibly due to the nature, strength, amount and distribution of the acid and basic surface sites.

For further examinations, we have selected Ben as a solid additive; for comparison some reactions were also carried out using Al<sub>2</sub>O<sub>3</sub> in order to have insight into the role of the layered structure and cation-exchanger character of the former. The influence of the reaction time is plotted in Fig. 1. Close to complete Conv was reached in 8 h using Ben in <sup>i</sup>Pr<sub>2</sub>O, whereas 16 h were needed in EtOAc. In the latter solvent Ben afforded a higher rate compared to Al<sub>2</sub>O<sub>3</sub>. Rates calculated from Convs obtained between 2 and 4 h (or 1–2 h in <sup>i</sup>Pr<sub>2</sub>O) in the presence of Ben decreased from 0.054 to 0.033 mmol h<sup>-1</sup> by changing the solvent from <sup>i</sup>Pr<sub>2</sub>O to EtOAc, whereas in the former solvent Al<sub>2</sub>O<sub>3</sub> afforded a lower value (0.024 mmol h<sup>-1</sup>). The lower initial rates obtained in the first 2 or 1 h (in EtOAc or <sup>i</sup>Pr<sub>2</sub>O, respectively, see values in Fig. 1) of each reaction indicated an induction period, which may be attributed to the formation of the active surface sites in the early stages of the reactions. The ees were similar in these reactions, 97% was obtained, which slightly increased (to 98%) at higher Convs of **2a** (>20–40%).

In a study on the effect of the inorganic additive amount, disparate reaction times were applied in the two solvents, due to the above determined significant rate differences (Fig. 2). Convs increased by raising the amount of the additive. In EtOAc in 16 h reactions 25 mg Ben was sufficient to reach high Conv and 50 mg afforded complete transformation of **2a**, whereas 100 mg Al<sub>2</sub>O<sub>3</sub> was necessary to obtain a similar result. In reactions in <sup>i</sup>Pr<sub>2</sub>O over 90% Conv was obtained in 6 h when 200 mg Ben was used. In contrast with that observed in EtOAc, in <sup>i</sup>Pr<sub>2</sub>O less Al<sub>2</sub>O<sub>3</sub> (100 mg) was needed to reach high Conv, compared to Ben (see the ESI,†

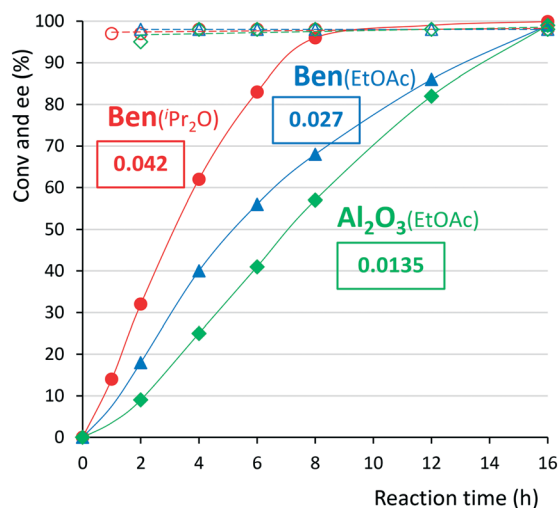


**Fig. 1** Effect of reaction time on Conv (closed symbols) and ee (open symbols) obtained in the addition of **1a** to **2a** catalysed by L-Phe in the presence of Ben or Al<sub>2</sub>O<sub>3</sub>. Reaction conditions: 0.03 mmol L-Phe, 1.2 mmol **1a**, 0.3 mmol **2a**, 100 mg additive, 1 cm<sup>3</sup> solvent, rt; Ben in <sup>i</sup>Pr<sub>2</sub>O (●, ○), Ben in EtOAc (▲, △), Al<sub>2</sub>O<sub>3</sub> in EtOAc (◆, ◇); the framed initial rate values (mmol h<sup>-1</sup>) were calculated at 1 h (<sup>i</sup>Pr<sub>2</sub>O) or 2 h (EtOAc).



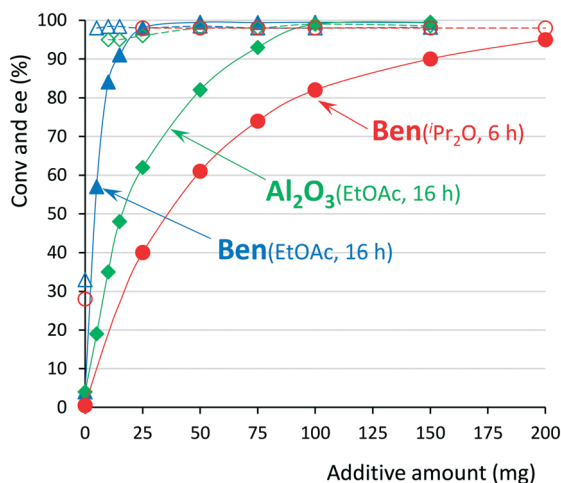


**Fig. 2** Effect of the inorganic additive amount on Conv (closed symbols) and ee (open symbols) obtained in the addition of **1a** to **2a** catalysed by *L*-Phe. Reaction conditions: 0.03 mmol *L*-Phe, 1.2 mmol **1a**, 0.3 mmol **2a**, 1 cm<sup>3</sup> solvent, rt; Ben in EtOAc, 16 h ( $\blacktriangle$ ,  $\triangle$ ), Al<sub>2</sub>O<sub>3</sub> in EtOAc, 16 h ( $\blacklozenge$ ,  $\lozenge$ ), Ben in <sup>*i*</sup>Pr<sub>2</sub>O, 6 h ( $\bullet$ ,  $\circ$ ).

Fig. S1). The ee values obtained were high in the experiments in which an additive was used (98%), slightly lower ees were reached at low Conv in EtOAc.

The effect of the *L*-Phe amount was examined in EtOAc (ESI,† Fig. S2). 10 mol% *L*-Phe was necessary to reach full transformation of **2a**; however, close to 60% Conv was reached with 5 mol% amino acid. Decreasing the reaction temperature to 5 °C lowered the Conv, whereas, at higher temperature in EtOAc high Convs could be obtained in shorter reactions without significant alteration of the ee. Thus, with 50 mg Ben at 50 °C in 4 and 6 h, 85% and 94% Convs and 97% ees were reached.

Similarly, decreasing the amount of the aldehyde lowered the Conv without altering the ee (ESI,† Fig. S3). With only 10% excess of **1a** compared to **2a** (0.33 mmol, 1.1 equivalent, eq.) close to 70% Conv was obtained. This value increased to higher than 80% and 90% with 2 and 3 eq. of **1a**, respectively. The Conv decreased with 5 eq. of **1a**, probably due to poisoning of the surface by more extensive side product formation. While keeping the amounts of reactants at the same values the solvent amount could be decreased to 0.25 cm<sup>3</sup> using Ben without significantly altering the Conv or ee (ESI,† Fig. S4). Higher amounts of solvent led to a decrease in Conv, due to the decrease in the concentration of the reactants and/or catalytically active sites. By increasing the maleimide amount, the Conv decreased (ESI,† Fig. S5) though the ratio of the reactants was kept constant. This allowed us to calculate the overall reaction rates, which increased with the **2a** concentration. However, a detailed kinetic analysis of the reaction necessitates determination of the effect of the components' concentration on the initial rates. As our aim during this study was to find the appropriate conditions for synthetic application of this catalytic system, further kinetic studies will be carried out latter and will be reported in our forthcoming publications.

The effect of the structure of the chirality source was examined using several natural and some synthetic amino acids (see ESI,† Fig. S6). Initial results with 50 mg Ben in EtOAc at 50 °C (ESI,† Table S1) showed that *L*-Phe was the most active and enantioselective catalyst; however, high ee (over 90%) can be reached with several other amino acids (*L*-Trp, *D*-PhGly, *D*-ChGly, *L*-Val, *L*-Leu, *L*-Ile, *L*-<sup>*L*</sup>Leu, *L*-Cys, *L*-Met), with the synthetic *L*-<sup>*L*</sup>Leu affording the same value as *L*-Phe. Previously it was observed that the ee is slightly better at high Convs; moreover, in the reaction carried out at rt with *L*-Phe the results improved (ESI,† Table S1). Thus, next we performed 24 h reactions with 200 mg Ben in <sup>*i*</sup>Pr<sub>2</sub>O at rt (Table 3). Under these conditions, several compounds provided both Conv and ee values over 90% (*L*-Trp, *L*-Val, *L*-Leu, *L*-Ile, *L*-<sup>*L*</sup>Leu, *L*-Met). *D*-PhGly and *D*-ChGly afforded the opposite product enantiomer in excess compared to *L*-Phe (ee > 90%). The poor results achieved with *L*-Phe methyl ester (*L*-PheMe) or *N*-protected *Z*-*L*-Phe indicated that both the carboxylic acid and the amine groups are necessary to reach good performances. The latter forms the enamine intermediate, through which primary amine catalysed reactions occur,<sup>17,36</sup> whereas the former may anchor and activate the maleimide, similar to what was suggested in reactions catalysed by amino acid salts.<sup>38,39</sup> Secondary amines (Me-*L*-Ile, *L*-Pro) gave poor results, probably due to the low rate of enamine formation, which during the addition of **1a** to  $\beta$ -nitrostyrene also required harsher reaction conditions.<sup>70</sup>

**Table 3** Michael addition of **1a** to **2a** catalysed by various amino acid derivatives in the presence of Ben<sup>a</sup>

Entry	Amino acid	Conv <sup>b</sup> (%)	ee <sup>c</sup> (%)
1 <sup>d</sup>	<i>L</i> -Phe	95	98 ( <i>S</i> )
2	<i>L</i> -Phe	>99	98 ( <i>S</i> )
3	<i>L</i> -PheMe <sup>e</sup>	50	57 ( <i>S</i> )
4	<i>Z</i> - <i>L</i> -Phe	1.5	8 ( <i>S</i> )
5	<i>L</i> -Trp	98	98 ( <i>S</i> )
6	<i>L</i> -His	93	83 ( <i>S</i> )
7	<i>D</i> -PhGly	85	91 ( <i>R</i> )
8	<i>D</i> -ChGly	82	95 ( <i>R</i> )
9	<i>L</i> -Ala	72	81 ( <i>S</i> )
10	<i>L</i> -Val	90	96 ( <i>S</i> )
11	<i>L</i> -Leu	98	95 ( <i>S</i> )
12	<i>L</i> -Ile	98	98 ( <i>S</i> )
13	Me- <i>L</i> -Ile	8	0
14	<i>L</i> - <sup><i>L</i></sup> Leu	>99	98 ( <i>S</i> )
15	<i>L</i> -Ser	63	74 ( <i>S</i> )
16	<i>L</i> -Cys	83	80 ( <i>S</i> )
17	H <sub>2</sub> N- <i>D</i> -Ala <sup>e</sup>	73	43 ( <i>R</i> )
18	<i>L</i> -Thr	50	87 ( <i>S</i> )
19	<i>L</i> -Met	>99	95 ( <i>S</i> )
20	<i>L</i> -Asn	44	74 ( <i>S</i> )
21	<i>L</i> -Asp	74	31 ( <i>S</i> )
22	<i>L</i> -Lys <sup>e</sup>	96	22 ( <i>S</i> )
23	<i>L</i> -Arg <sup>e</sup>	43	72 ( <i>S</i> )
24	<i>L</i> -Pro	2	5 ( <i>S</i> )

<sup>a</sup> Reaction conditions: 0.03 mmol amino acid, 1.2 mmol **1**, 0.3 mmol **2a**, 200 mg Ben, 1 cm<sup>3</sup> <sup>*i*</sup>Pr<sub>2</sub>O, rt, 24 h. <sup>b</sup> Determined by GC. <sup>c</sup> ee and configuration of the excess enantiomer obtained by GC. <sup>d</sup> 6 h reaction. <sup>e</sup> Used as HCl salt.



Additional acidic, basic or hydrogen-bond donor groups on the primary amino acid chain had detrimental effects both on the Conv and ee, as indicated by results obtained applying L-His, L-Ser, L-Cys, H<sub>2</sub>N-D-Ala, L-Thr, L-Asn, L-Asp, L-Lys and L-Arg. While a second amine functional group (H<sub>2</sub>N-D-Ala, L-Lys) may catalyse unselectively the addition, an additional acidic group (L-Asn, L-Asp) probably affects the adsorption mode of the amino acid on the Ben surface and may interact with the maleimide, perturbing the formation of an efficient transition state. Similarly, hydrogen-bond donor hydroxyl and thiol groups (L-Ser, L-Cys, L-Thr) may influence the interaction with both the surface and **2a**. The methylthio group in L-Met had less effect probably due to the distance from the chiral scaffold, affording similar results to amino acids having hydrocarbon chains.

An increase in the bulkiness of the aliphatic hydrocarbon unit raised both the Conv and ee; however, even L-Leu could not equal the performance of L-Phe (Table S1<sup>†</sup>), though, under the conditions applied in reactions presented in Table 3 they gave identical results. The same tendencies were obtained in reactions in EtOAc at rt using the Al<sub>2</sub>O<sub>3</sub> additive (ESI<sup>†</sup>, Table S2).

### Scope of the enantioselective catalytic system

With the *in situ* formed asymmetric heterogeneous catalyst obtained by the addition of Ben to the slurry containing a catalytic amount of L-Phe we have examined the scope of the system by carrying out the addition of **1a** to various *N*-substituted maleimide derivatives (see their structures in Fig. 3). Results of experiments carried out in EtOAc with 50 mg Ben both at rt and at 50 °C using derivatives bearing aromatic moieties are summarized in Table 4.

At rt 16 h were necessary to reach full Conv with *N*-benzylmaleimide **2a**; however, this was not sufficient to transform all the examined derivatives (except **2i**, **2j**, **2l** and

**2p**), thus longer reaction times (22, 28 or 44 h) were applied. However, at 50 °C most of the maleimides were converted in 6 h (except **2g**). With the exception of the  $\alpha$ -substituted compounds (*rac*-**2f**, *S*-**2f**, *R*-**2f**), benzylmaleimides were completely transformed and high ees were obtained (96–98%) (Table 4, entries 1–5), only the reaction of the 4-methoxybenzyl derivative (**2b**) had to be extended at rt to 28 h (entry 2).

The chiral centres of the optically pure *N*- $\alpha$ -methylbenzylmaleimides were not affected during reactions, and adducts were formed enantioselectively without racemization at the benzylic position (entries 7, 8), whereas the racemic compound afforded the diastereomers in equal amounts, *i.e.* no kinetic resolution occurred (after 6 h at 34% Conv the dr was 50/50, not included). Distancing the phenyl ring from the imide moiety (**2g**) led to a lower reaction rate (entry 9), thus a longer time was needed, however, the ee approached those reached in reactions of benzyl derivatives.

*N*-Phenylmaleimide (**2h**) and its substituted derivatives (**2i**–**2p**) were also transformed enantioselectively (95–97%) with the exception of the 4-methoxy derivative (**2i**), which afforded a slightly lower (89%) ee (Table 4, entries 10–18). Substituents on the phenyl ring affected the rate, *i.e.* the time necessary to reach high Conv. Thus, the *ortho* substituents on the phenyl ring had a detrimental effect on the rate, leading to Convs which hardly exceeded 90% at rt even after 44 h (entries 16, 17).

Further, we have examined the Michael addition of **1a** to maleimides bearing aliphatic *N*-substituents (Table 5). Based on the reaction of **2g** we expected that these derivatives will react slower, compared to *N*-phenyl or *N*-benzyl compounds. Indeed, maleimides having linear *N*-alkyl substituents needed 44 h at rt or 16 h at 50 °C to reach good Convs (Table 5, entries 2–6), except **4a** and **4g** (entries 1, 7). For reacting the former (*N*-methylmaleimide) one day was sufficient at rt, whereas for the latter (*N*-dodecylmaleimide) longer times (72

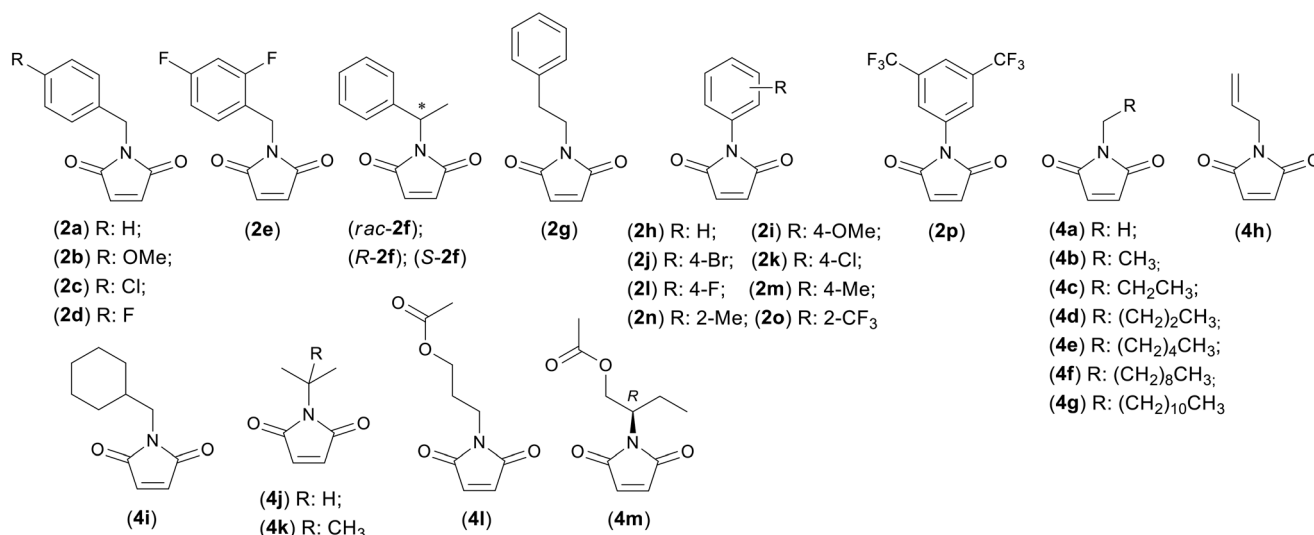
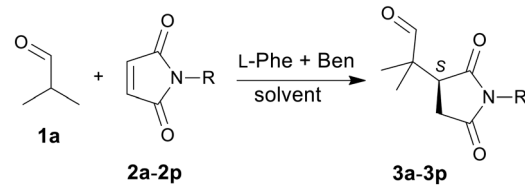


Fig. 3 Structures of the *N*-substituted maleimides used to study the scope of the L-Phe + Ben catalytic system.



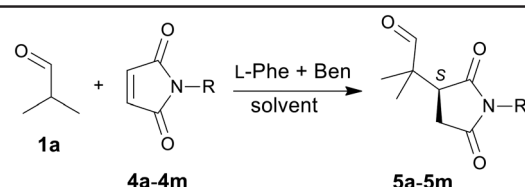
**Table 4** Asymmetric Michael addition of **1a** to *N*-substituted maleimides **2a–2p** catalysed by L-Phe in the presence of Ben<sup>a</sup>


Entry	Product	Conv (yield) <sup>b</sup> (%)	ee <sup>b</sup> (%)
1	<b>3a</b>	>99 (92); <sup>c</sup> 96	98.5; 97.5
2	<b>3b</b>	>99 (90); <sup>d</sup> 99	97.5; 97.5
3	<b>3c</b>	>99 (88); 98	97.5; 97
4	<b>3d</b>	>99 (90); 99	97.5; 97
5	<b>3e</b>	99 (91); 92	97; 96.5
6	<b>3f</b>	72, dr 50/50 <sup>e</sup>	98, 98
7 <sup>f</sup>	<b>3f</b>	92 (80); 89	98; 98
8 <sup>g</sup>	<b>3f</b>	90 (78); 84	98; 97
9	<b>3g</b>	94; <sup>h</sup> 99 (88) <sup>i</sup>	96.5; 95.5
10	<b>3h</b>	99 (90); <sup>d</sup> 99	97; 96
11	<b>3i</b>	96 (85); <sup>c</sup> 97	89; 89
12	<b>3j</b>	>99 (90); <sup>c</sup> >99	95; 94
13	<b>3k</b>	>99 (88); ne	95; ne
14	<b>3l</b>	>99 (88); <sup>c</sup> >99	96; 94
15	<b>3m</b>	98 (88); ne	96; ne
16	<b>3n</b>	93 (80); <sup>h</sup> ne	96; ne
17	<b>3o</b>	92 (80); <sup>h</sup> ne	95; ne
18	<b>3p</b>	>99 (88); <sup>c</sup> ne	95; ne

<sup>a</sup> Reaction conditions: 0.03 mmol L-Phe, 0.3–1.2 mmol **1a**, mmol **2a–2p**, 50 mg Ben, 1 cm<sup>3</sup> EtOAc; ne: not examined. <sup>b</sup> Conversions (Conv) and enantiomeric excesses (ee, excess of *S* enantiomers) determined by GC at rt (22 h); and at 50 °C (6 h), in brackets the isolated yields. <sup>c</sup> 16 h reaction at rt. <sup>d</sup> 28 h at rt. <sup>e</sup> dr: diastereomeric ratio in the reaction of *rac*-**2f** at rt. <sup>f</sup> Using *S*-**2f**, product with *S,S* configuration. <sup>g</sup> Using *R*-**2f**, product with *S,R* configuration. <sup>h</sup> 44 h at rt. <sup>i</sup> 16 h at 50 °C.

h at rt, 24 h at 50 °C) were necessary. Slightly better transformations were obtained with the *N*-allyl and the *N*-(3-acetoxypropyl) compounds (**4h** and **4i**, entries 8, 12)

compared to the *N*-propyl **4c**. The compound having cyclohexyl (**4i**) instead of the phenyl ring of the *N*-benzylmaleimide reacted much slower than **2a**. Maleimides

**Table 5** Asymmetric Michael addition of **1a** to *N*-substituted maleimides **4a–4m** catalysed by L-Phe in the presence of Ben<sup>a</sup>


Entry	Product	Conv (yield) <sup>b</sup> (%)	ee <sup>b</sup> (%)
1	<b>5a</b>	80; <sup>c</sup> 85 (70)	96; 95
2	<b>5b</b>	88; 95 (82)	96; 95
3	<b>5c</b>	87 (75); 84	97; 95
4	<b>5d</b>	83 (70); 85	97; 95
5	<b>5e</b>	79; 91 (80)	97; 96
6	<b>5f</b>	88; 94 (80)	96; 95
7	<b>5g</b>	95; <sup>d</sup> 97 (85) <sup>e</sup>	96; 96
8	<b>5h</b>	96; 99 (86)	97; 96
9	<b>5i</b>	92 (80); <sup>d</sup> 84	96; 95
10	<b>5j</b>	97 (85); <sup>d</sup> 86 <sup>e</sup>	97; 95
11	<b>5k</b>	42; <sup>d</sup> 78 (65) <sup>f</sup>	96; 94
12	<b>5l</b>	98; 99 (88)	96; 95
13	<b>5m</b>	88; <sup>d</sup> 94 (80) <sup>g</sup>	95; 94

<sup>a</sup> Reaction conditions: 0.03 mmol L-Phe, 1.2 mmol **1a**, 0.3 mmol **4a–4m**, 50 mg Ben, 1 cm<sup>3</sup> EtOAc. <sup>b</sup> Conversions (Conv) and enantiomeric excesses (ee, *S* excess enantiomer) determined by GC in reactions at rt (44 h); and at 50 °C (16 h), in brackets the isolated yields. <sup>c</sup> 22 h reaction at rt. <sup>d</sup> 72 h at rt. <sup>e</sup> 24 h at 50 °C. <sup>f</sup> 72 h at 50 °C. <sup>g</sup> No racemization of the *N* substituent, product with *S,R* configuration.



with  $\alpha$ -branched aliphatic substituents (**4j**, **4m**) also required longer reactions; moreover *N*-<sup>t</sup>Bu **4k** afforded only 78% Conv even after 72 h at 50 °C. In all these reactions high ee values (94–97%) were reached at rt, slightly higher than those at 50 °C.

Accordingly, the addition of **1a** to a large variety of *N*-substituted maleimides may be carried out enantioselectively using the catalyst formed from *L*-Phe and Ben. Next, we have examined the effect of the structure of the nucleophile using aldehydes (**1b–1f**) and ketones (**1g–1i**) (see ESI,† Fig. S7 for structures) in reactions with **2a**, **4a–4d**, **4j** as electrophiles. The structure of the products and the results obtained are shown in Fig. 4 and Table 6, respectively. In order to shorten the reaction time, we have used 100 mg Ben in these experiments. The additions of cyclohexanecarboxaldehyde (**1b**) occurred with high Convs and similarly good ees to those of **1a** (Table 6, entries 1–4). The other two racemic  $\alpha$ -branched aldehydes, *i.e.* 2-methylbutanal (**1c**) and 2-ethylhexanal (**1d**), also afforded the Michael adducts with high ee, the latter giving a lower Conv even after 2 days (entries 5, 6). In these reactions, the aldehyde enantiomers reacted with similar rates leading to  $\approx$ 60/40 diastereomeric ratios.

Aldehydes without  $\alpha$ -substituents, such as propanal (**1e**) and 3-methylbutanal (**1f**), were even less reactive and needed 5 days at 50 °C to obtain over 70% Convs (entries 7, 8). The lower transformation rates observed in reactions of these compounds may be ascribed to the lower nucleophilicity of the enamine intermediate compared to those formed from  $\alpha$ -branched aldehydes.<sup>36</sup> The ees decreased in these reactions to  $\leq$ 90%, whereas the dr slightly improved in the reaction of

the  $\beta$ -branched **1f**, probably due to the steric effect of the aliphatic chain. The addition of ketones proceeded at 50° in 5 or 7 days (entries 9–11); however, these reactions afforded similarly low drs ( $\approx$ 60/40) as the aldehydes and much lower ees.

### Recycling of the chiral solid material

The outstanding catalytic activities and enantioselectivities obtained in the Michael addition of  $\alpha$ -branched aldehydes to maleimides with the catalyst formed using *L*-Phe and inorganic oxides indicated that the latter materials play an essential role in catalysing the asymmetric reaction. Thus, it is probable that the catalytic reaction takes place on the surface of the material, similar to what was suggested to occur during the addition of aldehydes to  $\beta$ -nitrostyrenes promoted by amino acids adsorbed on the Lap surface.<sup>70</sup> Accordingly, a heterogeneous chiral catalyst was formed *in situ*. We have tested the recyclability of this chiral solid in the addition of **1a** to **2a**. Initially, we examined the use of 200 g Ben at rt in <sup>i</sup>Pr<sub>2</sub>O, which needed only 6 h to obtain 95% Conv (Fig. 5).

A gradual decrease in the Conv from the 3rd use led to lower than 60% transformation of **2a** in the 5th run. The activity could be partially restored (to over 80% Conv), by addition of half amount of *L*-Phe compared to that initially applied (see arrows in Fig. 5). In all these experiments high ees (98%) were obtained. These results confirmed that the surface of the oxide is catalytically active and acts as a heterogeneous catalyst. Although during recycling the number of the active surface sites decreases, the remaining active sites are similarly stereoselective to those engaged during the first use, *i.e.* incorporate surface-immobilized amino acids.

The activity decrease may be explained both by desorption of the amino acid from the surface (leaching) and by poisoning of the solid material by adsorbed reactants, products and side-products, such as those resulting from condensations of the excess aldehyde. Thus, the addition of the amino acid during reuse could restore only partially the activity of the catalyst. Moreover, when the reuse was carried out with the addition of 5 mol% *L*-Phe in each run from the beginning, the Conv also decreased to 80% and was maintained at 80–90% until the 8th use (Fig. 5). Accordingly, the above-mentioned poisoning should be responsible for the slightly lowered Conv rather than desorption of the chirality source.

In continuation, we attempted to prepare *ex situ* the chiral heterogeneous catalyst. In their catalytic tests, low amounts of solids were applied both at rt and 50 °C (Table 7). Under these conditions, the *in situ* prepared catalyst gave better Conv in <sup>i</sup>Pr<sub>2</sub>O compared to EtOAc at rt, whereas at 50 °C close to full Convs were reached (entries 1, 2). In EtOAc if the reaction carried out at 50 °C was stopped after 1 h, in the liquid phase the Conv hardly increased following another 5 h under the same conditions (entries 3, 4). The separated solid

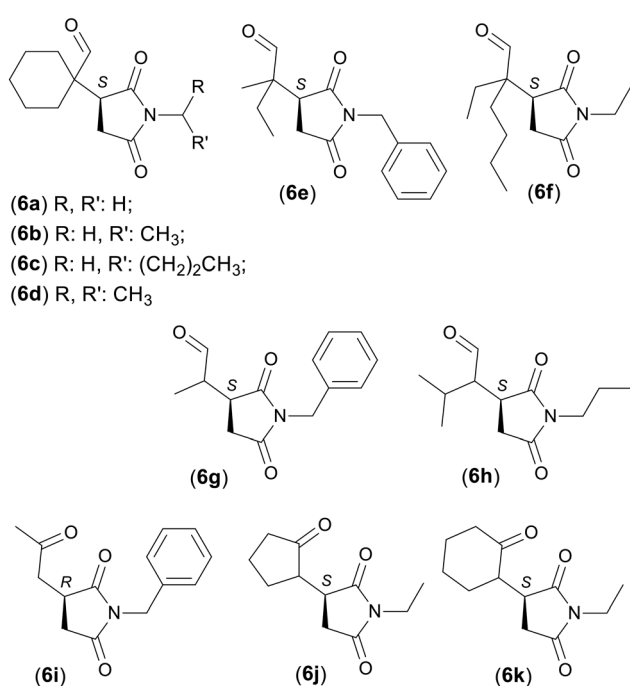
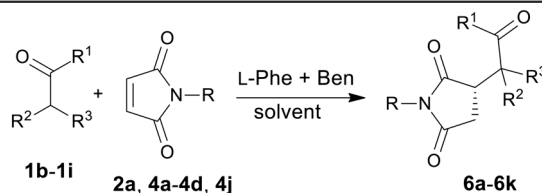


Fig. 4 Structure of Michael adducts obtained in reactions of various carbonyl compounds.



**Table 6** Asymmetric Michael addition of various carbonyl compounds to *N*-substituted maleimides catalysed by *L*-Phe in the presence of Ben<sup>a</sup>

Entry	Product	Conv (yield) <sup>b</sup> (%)	ee <sup>b</sup> (%)
1	6a	>99 (90); >99	99; 99
2	6b	>99 (88); 99	97; 97
3	6c	97 (85); 99 <sup>c</sup>	97; 95
4	6d	93 (80); 99 <sup>c</sup>	98; 94
5	6e	99 (86); 99	60/40, 99, 97 <sup>d</sup>
6	6f	78 (65) <sup>e</sup>	62/38, 98, 98 <sup>d</sup>
7	6g	76 (60) <sup>f</sup>	52/48, 90, 88 <sup>d</sup>
8	6h	65; <sup>g</sup> 77 (62) <sup>f</sup>	66/34, 87, 88 <sup>d</sup>
9	6i	96 (80) <sup>h</sup>	30
10	6j	72 (55) <sup>f</sup>	60/40, 54, 18 <sup>d</sup>
11	6k	62 (50) <sup>f</sup>	58/42, 26, 14 <sup>d</sup>

<sup>a</sup> Reaction conditions: 0.03 mmol *L*-Phe, 1.2 mmol carbonyl compound, 0.3 mmol maleimide derivative, 100 mg Ben, 1 cm<sup>3</sup> EtOAc, rt 24 h; 50 °C 16 h. <sup>b</sup> Conversions and enantiomeric excesses (ee) determined by GC in reactions at rt (24 h); and 50 °C (16 h), in brackets the isolated yields. <sup>c</sup> 24 h at 50 °C. <sup>d</sup> Diastereomeric ratio and enantiomeric excesses (ee) obtained by GC analysis of the raw product. <sup>e</sup> At rt 48 h. <sup>f</sup> At 50 °C 5 days. <sup>g</sup> At rt 7 days. <sup>h</sup> At 50 °C 7 days.

reused in a subsequent reaction afforded similar results to those obtained with the use of the fresh, *in situ* formed catalyst (entries 2, 5). These experiments confirmed the heterogeneous nature of the *in situ* formed active catalyst.

The hybrid materials prepared *ex situ* by *L*-Phe deposition on Ben at rt in both solvents, EtOAc (*L*-Phe–Ben1) and <sup>i</sup>Pr<sub>2</sub>O (*L*-Phe–Ben2), respectively afforded similar results to those obtained with the *in situ* formed catalysts in the corresponding solvents (entries 2, 7 and 1, 8). However, the one prepared in EtOAc and used in <sup>i</sup>Pr<sub>2</sub>O afforded

intermediate results (entry 6). Accordingly, the chiral materials may be prepared *ex situ* as well; however, the solvent used in the preparation of these materials may affect the activity of the catalyst. Pre-adsorption of *N*-benzylmaleimide, 2a, on Ben in either solvent gave materials, which by addition of *L*-Phe to the slurry performed similarly to *L*-Phe–Ben1 prepared in EtOAc (compare entries 9, 10 to 6). However, these Convs were lower than that

**Table 7** Application of *ex situ* prepared hybrid materials in the Michael addition of 1a to 2a<sup>a</sup>

Entry	Catalyst	Conv <sup>b</sup> (%)	ee <sup>b</sup> (%)
1	Ben + <i>L</i> -Phe	61; >99	97.5; 97
2	Ben + <i>L</i> -Phe <sup>c</sup>	32; 96	98; 97.5
3	Ben + <i>L</i> -Phe <sup>d</sup>	28	96
4	Stirring the liquid phase <sup>d</sup>	33	96
5	Reuse of the solid <sup>d</sup>	95	96.5
6	<i>L</i> -Phe–Ben1 <sup>e</sup>	46; 97	97; 97
7	<i>L</i> -Phe–Ben1 <sup>e, c</sup>	32; 93	97; 97
8	<i>L</i> -Phe–Ben2 <sup>f</sup>	61; >99	97; 97
9	2a–Ben <sup>e</sup> + <i>L</i> -Phe	48; 99	96; 97.5
10	2a–Ben <sup>f</sup> + <i>L</i> -Phe	47; >99	97; 97.5
11	1a–Ben <sup>e</sup> + <i>L</i> -Phe	51; 98	97; 97
12	S-3a–Ben <sup>e</sup> + <i>L</i> -Phe	46; 94	97; 96

<sup>a</sup> Reaction conditions: 55 mg *ex situ* prepared hybrid material or 50 mg Ben + 0.03 mmol *L*-Phe, 1.2 mmol 1a, 0.3 mmol 2a, 1 cm<sup>3</sup> <sup>i</sup>Pr<sub>2</sub>O, 6 h. <sup>b</sup> Conversions and enantiomeric excesses (ee) obtained in reactions at rt; and 50 °C determined by GC, excess of *S* enantiomer. <sup>c</sup> Reaction in 1 cm<sup>3</sup> EtOAc. <sup>d</sup> Reaction at 50 °C stopped after 1 h, centrifuged, followed by stirring of the supernatant at 50 °C 5 h and reuse of the solid using fresh reactants and EtOAc in a 6 h reaction. <sup>e</sup> Material prepared *ex situ* by stirring 500 mg Ben and 0.3 mmol organic compound (*L*-Phe or 1a or 2a or S-3a) in 10 cm<sup>3</sup> EtOAc at rt for 6 h. <sup>f</sup> The hybrid material was prepared in 10 cm<sup>3</sup> <sup>i</sup>Pr<sub>2</sub>O.

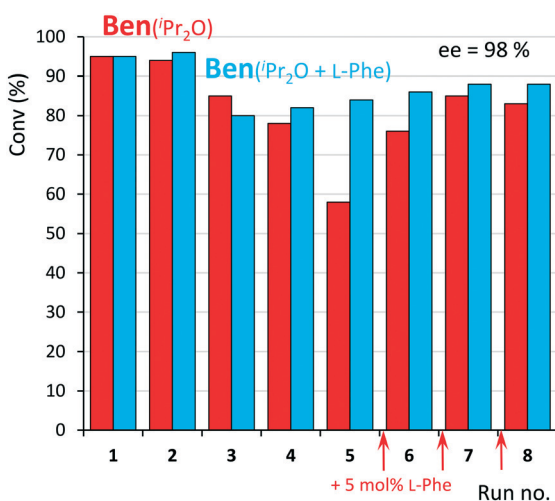


**Fig. 5** Recycling of the *in situ* formed chiral catalysts in the addition of 1a to 2a. Reaction conditions: 0.03 mmol (10 mol%) *L*-Phe, 1.2 mmol 1a, 0.3 mmol 2a, 200 mg Ben, 1 cm<sup>3</sup> <sup>i</sup>Pr<sub>2</sub>O, rt, 6 h; red columns without addition of *L*-Phe (unless marked with arrows), blue columns with addition of 5 mol% *L*-Phe during each recycling.



obtained with L-Phe–Ben2, thus, when  $^1\text{Pr}_2\text{O}$  is used both in the deposition and in the reaction, the adsorbed **2a** decreases the activity.

Similarly, the materials obtained by pre-adsorption of **1a** or **S-3a** were less active than L-Phe–Ben2. Accordingly, pre-adsorption of the reagents or the product hinders to some extent the adsorption of the amino acid, leading to a decrease in the number of the active surface sites. This confirms that the reaction occurs on the surface and gives a plausible explanation of the slight decrease in the Conv observed even when the amino acid is added in each recycling run.

### Characterization of the chiral heterogeneous catalyst

The above described *in situ* formed or *ex situ* prepared chiral hybrids were examined by various methods in order to determine their structure and stability. Initially, we investigated the amount of the deposited L-Phe by measuring the amount of amino acid left in solution using UV-vis spectroscopy (for spectra and calibration see ESI,† Fig. S8–S11). Due to the high UV cut-off wavelength and the low solubility of L-Phe in the applied solvents, we used MeOH in these experiments. In MeOH the reaction of **1a** and **2a** was complete in the presence of Lap and afforded moderate ee (Table 1), indicating that the chiral hybrid catalyst is formed. Results using 100 mg Ben are shown in Fig. 6 (see ESI,† Fig. S12 for results with 100 mg  $\text{Al}_2\text{O}_3$ ).

Even the lowest amount of L-Phe (0.0075 mmol) was not completely adsorbed over Ben; however, increasing the L-Phe amount led to a linear increase of the deposited amino acid quantity (Fig. 6). The amount of the amino acid decreased

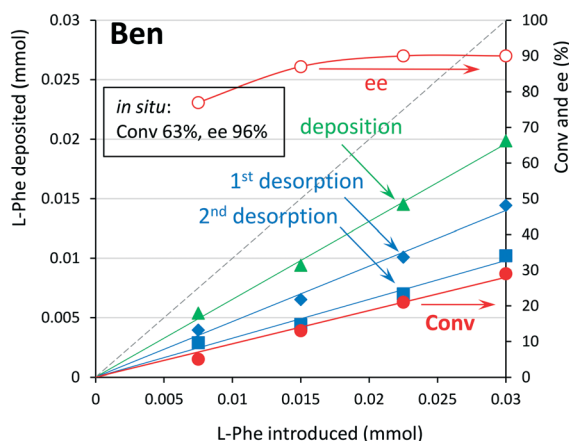


**Fig. 6** Amount of L-Phe deposited on 100 mg Ben from 1 cm<sup>3</sup> MeOH determined by UV-vis spectroscopy; ▲ L-Phe amount included after 2 h stirring at rt, ◆ L-Phe amount remained following another 2 h washing using 1 cm<sup>3</sup> MeOH, ■ L-Phe amount remained following a 2nd 2 h washing using 1 cm<sup>3</sup> MeOH. Conv ● and ee ○ obtained applying the final materials as catalysts in the addition of **1a** to **4a**. Reaction conditions: 1.2 mmol **1a**, 0.3 mmol **4a**, 1 cm<sup>3</sup> EtOAc, rt, 16 h; the result obtained under identical conditions with the catalyst formed *in situ* using 0.03 mmol L-Phe is given in the frame.

after repeated washing of the solid with MeOH, leading to desorption of about one third of the incorporated quantities by each treatment. In contrast,  $\text{Al}_2\text{O}_3$  adsorbed higher amounts of L-Phe, and following washings with MeOH the removed quantities were also smaller (Fig. S12†). The four hybrid materials obtained after washings using Ben gave proportionally increasing conversions of **4a** (in reaction with **1a** in EtOAc) with the increasing quantity of the amino acid (Fig. 6). However, even with the material containing the highest amount of L-Phe the Conv was lower compared to that obtained in the reaction applying the *in situ* addition method. A similar trend was observed using the hybrid materials prepared from  $\text{Al}_2\text{O}_3$  (Fig. S12†). The ees were also slightly lower compared to the *in situ* use of the components; however, over a certain amount of deposited L-Phe, the ee values did not change. According to these experiments the deposited L-Phe forms surface chiral sites able to catalyse the asymmetric Michael addition and it is necessary to deposit a certain amount of amino acid for obtaining an efficient chiral solid catalyst.

The above results also showed that the amount of the deposited organic material is affected by the properties of the solid. The parent Ben has 0.9% CaO and 3.5%  $\text{Na}_2\text{O}$ , and thus, contains predominantly Na-montmorillonite beside the Ca-form. The thermal behaviour of the hybrid materials was investigated by thermogravimetric analysis (Fig. 7). The parent Ben was dehydrated until 150 °C ( $\approx 1$  wt%) with the gradual release of the interlayer water.<sup>76–78</sup> At higher

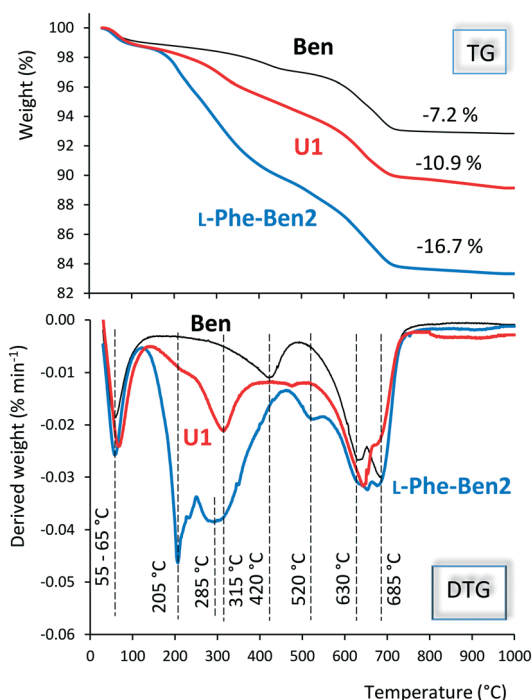


**Fig. 7** Thermogravimetric analysis (TG and DTG, 30 mg sample, heating rate 10 °C min<sup>-1</sup>) of Ben, L-Phe–Ben2 (Table 7) and the material resulted from 0.03 mmol L-Phe and 200 mg Ben in a 6 h reaction of **1a** and **2a** at 50 °C in 1 cm<sup>3</sup>  $^1\text{Pr}_2\text{O}$ , Conv > 99%, ee 96.5% (U1).



temperature dehydroxylation of the silicate lattice took place in two distinct events, the first peaking at 420 °C ( $\approx 2$  wt%), whereas the second gave a double peak at 630 and 685 °C in the DTG curve ( $\approx 4$  wt%).<sup>76–78</sup> Crystalline L-Phe decomposed over 220 °C giving two maxima in the DTG curve at 290 and 350 °C (ESI,† Fig. S13).

The *ex situ* prepared L-Phe–Ben2, following the initial loss of water and the remnant organic solvent ( $\approx 1.2$  wt%), showed a sharp peak with maximum at 205 °C followed by a broad one at 285 °C, attributable to the decomposition of L-Phe at lower temperature compared to pure L-Phe. The weight loss associated with these steps is  $\approx 9$  wt% (150–450 °C).

At higher temperatures the dehydroxylation of the material took place in two steps ( $\approx 6$  wt%), similar to the parent Ben; however, the first occurred at 520 °C (*vs.* 420). These results indicated the deposition of the amino acid. Moreover, a solid surface induced change of the deposited organic material also occurred, as evidenced by the shifted decomposition temperatures. According to these, the material prepared *ex situ* contained 9% L-Phe, which partially was transformed probably in phenylalaninate (Na or Ca) by interaction with Ben.

In contrast, the analysis of the *in situ* obtained material U1 showed that the major part of L-Phe decomposes giving a peak at 315 °C, which may be ascribed to the stronger bonding of the amino acid to the surface or/and to inclusion in the interlayer space. The amount of the L-Phe based on the weight loss (150–400 °C) was  $\approx 3$  wt%. The dehydroxylation of the silicate lattice occurred mostly over 550 °C. Although this step led to the same weight loss (6 wt%) as in the case of the previously examined materials, *i.e.* the amount of the –OH groups did not change, shifts in the maxima of the steps indicated the possible involvement of these groups in anchoring the organic material.

Accordingly, by thermogravimetry, we detected L-Phe bonded with different strengths in the examined materials. The main component of Ben is montmorillonite, a layered dioctahedral aluminosilicate with a 2:1 (TOT) structure having hydrated exchangeable cations compensating for the negative charge of the layers.<sup>73,74</sup> Although, under acidic conditions these cations may be exchanged by protonated amino acids,<sup>79</sup> in our study the amino acid may interact with these cations, forming intercalated and surface immobilized Na (or Ca) salt.

This motivated us to examine the hybrid materials by X-ray diffractometry (XRD). Diffractograms of selected materials are shown in Fig. 8. The basal distance  $d_{001}$  calculated according to Bragg's law using the 001 reflection in the diffractogram of Ben at  $2\theta$  7.04° was found to be 12.55 Å, corresponding to Na-montmorillonite. Reflections appeared in the XRD pattern (indexed according to the literature)<sup>80–82</sup> showed the presence of cristobalite (Crs,  $2\theta$  21.60°) as well.

According to the diffractograms of the *ex situ* prepared materials (L-Phe–Ben1 and L-Phe–Ben2) the basal distance of

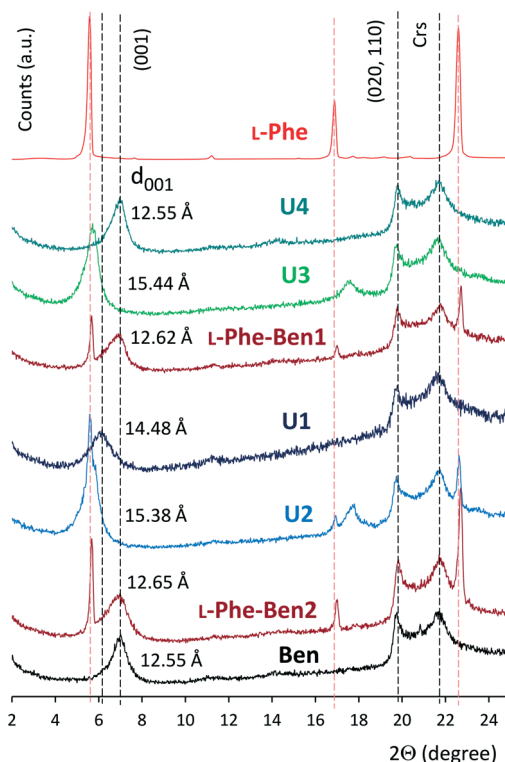


**Fig. 8** X-ray diffractograms of Ben, L-Phe, L-Phe–Ben1, L-Phe–Ben2, U1 (see Fig. 7) and several materials used in reactions of **1a** and **2a** in 1 cm<sup>3</sup> <sup>1</sup>Pr<sub>2</sub>O; U2: 55 mg of L-Phe–Ben2 after 12 uses in 6 h reactions at rt, last run Conv 37%, ee 96%, U3: 110 mg of L-Phe–Ben1 after 3 uses in 16 h reactions at rt, last run Conv 67%, ee 97.5%, U4: 55 mg of L-Phe–Ben1 after 4 uses in 6 h reactions at 50 °C, last run Conv 5%, ee 70%.

the montmorillonite hardly changed and reflections of crystalline L-Phe appeared, indicating the deposition of the amino acid crystallites on the surface of the inorganic solid. The material L-Phe–Ben1 prepared in EtOAc contained less amino acid compared to L-Phe–Ben2. Moreover, the latter material still contained crystalline L-Phe on the surface after 12 uses in <sup>1</sup>Pr<sub>2</sub>O (Fig. 8, U2), although the Conv decreased to 37% in the last use in the reaction of **1a** to **2a**. Interestingly, in this spent material (U2) the basal distance increased significantly to 15.38 Å ( $2\theta$  5.74°), indicating either the migration of the amino acid or deposition of organic residues into the interlamellar space during the reaction. Similarly, the basal distance increased (15.44 Å) following 3 uses of the material prepared *ex situ* in EtOAc (L-Phe–Ben1), meanwhile, the deposited crystalline L-Phe disappeared (Fig. 8, U3). However, when L-Phe–Ben1 was applied at 50 °C in 6 h reactions, after the 4th use the material lost its activity (Conv 5%) accompanied by a change in the basal distance of the montmorillonite (Fig. 8, U4), which became identical with that found in the parent Ben.

Interestingly, crystalline L-Phe was not detectable in the material obtained *in situ* (U1), giving >99% Conv and 96.5% ee, which upon reuse also gave good results. The interlamellar distance in this *in situ* formed hybrid was high



(14.48 Å) (Fig. 8, U1). Similar materials were obtained *in situ* in reactions carried out under other conditions with lamellae propped up to 14.52 or 14.57 Å (ESI,† Fig. S14, U6, U5), without containing deposited crystalline amino acid, however, all of these being active upon reuse.

According to the above results the active hybrid materials contained either deposited L-Phe crystallites without significantly changing the interlamellar distance of Ben (*ex situ*) or amino acid intercalated between the montmorillonite layers leading to a swelled hybrid material with increased interlamellar distance (*in situ*). Gradual leaching of the amino acid from this space led to loss of the activity with the simultaneous restoration of the initial distance between the lamellae. Thus, the sites active in the Michael addition contain the amino acid either adsorbed on the outer surface or intercalated in the interlamellar space. The deposited L-Phe crystallites may act as an amino acid supply compensating for the material leached from the above sites. However, the less accessible L-Phe included in the interlamellar space may also have the same role of compensating for the desorbed L-Phe, due to the difficulty of accessing the chiral material situated in the interlamellar space compared to the outer surface sites. The above interpretations are supported by the similar catalytic results obtained with Al<sub>2</sub>O<sub>3</sub>, lacking the lamellar structure.

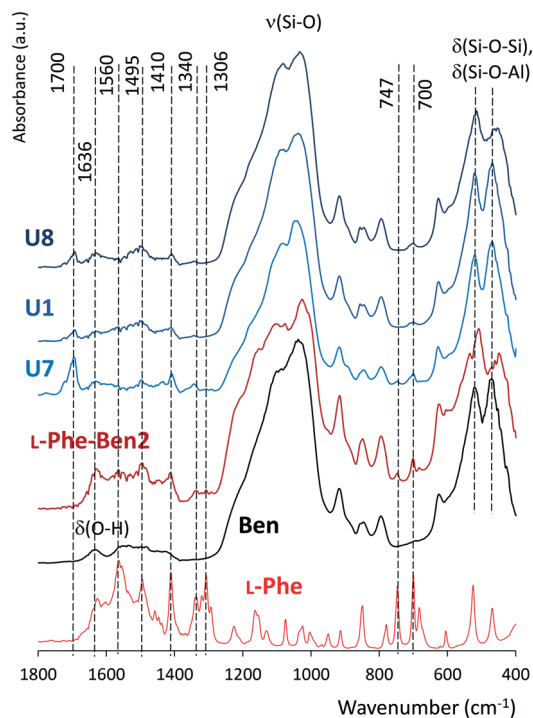


**Fig. 9** FT-IR spectra of L-Phe, Ben, L-Phe-Ben2 and three materials used in reactions of **1a** and **2a** in 1 cm<sup>3</sup> iPr<sub>2</sub>O: U1 (see Fig. 7); 55 mg of L-Phe-Ben2 after first use in a 6 h reaction at 50 °C, Conv 99%, ee 96.5%, (U7); *in situ* formed material from 200 mg Ben and 0.03 mmol L-Phe, in 6 h reactions at rt after ten uses, last run Conv 62%, ee 98% (U8).

The hybrid materials were also examined by Fourier transform infrared spectroscopy (FT-IR). Spectra of selected materials are presented in Fig. 9 (see full spectra in ESI,† Fig. S15) and compared with those of the parent Ben and L-Phe. In the FT-IR spectrum of Ben adsorption bands characteristic of the layered alumina silicate were detected, *i.e.* the stretching vibrations ( $\nu$ ) of the structural O–H, interlayer water and Si–O at 3616, 3466 (Fig. S15 and S16†) and 1035 cm<sup>-1</sup> and the bending vibrations ( $\delta$ ) of water, Si–O–Si and Al–O–Si bonds at 1636 cm<sup>-1</sup> and in the 400–600 cm<sup>-1</sup> region.<sup>78,82–86</sup> Bands at 1400–1480 cm<sup>-1</sup> were attributed to the presence of carbonates.<sup>87</sup>

In the spectrum of the *ex situ* prepared material (L-Phe–Ben2, Fig. 9 and S15 and S16†) additional bands were detected, which may be assigned to the deposited L-Phe in zwitterionic form.<sup>88,89</sup> Thus, the bands at 1625, 1560 and 1566, 1410 cm<sup>-1</sup> were attributed to the asymmetric and symmetric  $\delta(-\text{NH}_3^+)$  and  $\nu(-\text{COO}^-)$  vibrations, respectively. The bands at 1495, 1458 and those in the 1270–1370 cm<sup>-1</sup> interval are due to C–H bending and scissoring vibrations, which appeared in the spectrum of the material, along with the bands at 747 and 700 cm<sup>-1</sup>. The decrease in the intensity of the stretching vibrations of the interlamellar water (3466 cm<sup>-1</sup>, Fig. S16†) showed partial removal of the water, either by the included L-Phe or by the solvent; however, this led only to a small change in the interlamellar distance, as shown by XRD. In contrast, the band at 3616 cm<sup>-1</sup> attributed to the structural  $\nu(\text{O–H})$  increased, showing the hydration of the silicate layer upon depositing the amino acid. Bands characteristic to the N–H and C–H stretching vibrations (2800–3250 cm<sup>-1</sup>) were also detectable (Fig. S16†).

After one use of L-Phe–Ben2 at 50 °C (U7), absorption bands characteristic of the deposited L-Phe were still detectable, though they had lower intensity compared to the *ex situ* prepared material in agreement with the XRD results. Interestingly, the band at 3616 cm<sup>-1</sup> also decreased, which points to the involvement of the structural –O–H groups in the reaction. New bands around 1700 cm<sup>-1</sup> appeared in the spectrum of this material (U7), which may be due to the adsorption of reactants or products (including side-products) formed during the reaction (C=O group vibrations). This supposition was supported by the appearance of similar bands in the FT-IR spectra of samples prepared by adsorbing either one of the reactants or the purified product on Ben (not shown).

The spectrum of the material obtained by *in situ* addition of Ben and L-Phe (U1) was similar; however, the bands assigned to L-Phe were of lower intensity. According to XRD, no crystals of the amino acid are deposited on this material, thus, the FT-IR bands observed may be attributed to L-Phe adsorbed on the surface or included in the interlamellar space. The band at 3616 cm<sup>-1</sup> had lower intensity compared to Ben or L-Phe–Ben2, although slightly higher than that observed for U7. Similar changes were detected in the spectrum of the material obtained after ten uses (U8).



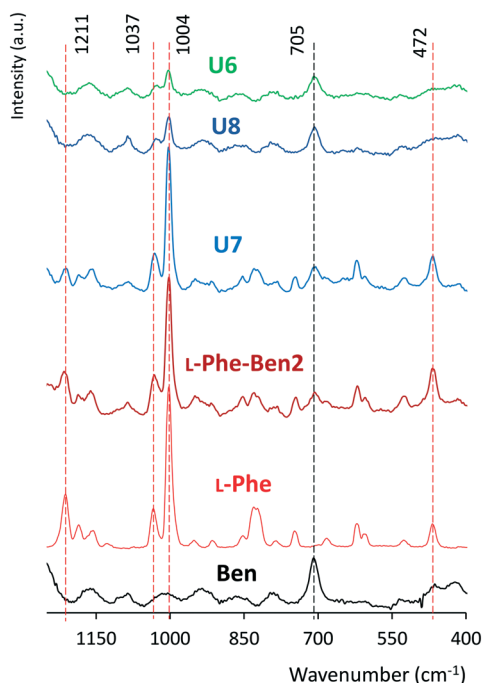


Fig. 10 Raman spectra of Ben, L-Phe, L-Phe-Ben2 and U6, U7, U8 (for identification of the used materials see Fig. 9 and ESI,† S14).

The materials surface was also examined by Raman spectroscopy using a 785 nm excitation laser of 100 mW. Selected ranges of the spectra are plotted in Fig. 10. The Raman spectrum of Ben is dominated by the band at 705  $\text{cm}^{-1}$  assigned to the  $\nu_1(a_1)$  vibration mode of  $\text{SiO}_4$  tetrahedra.<sup>90,91</sup> In the selected region (400–1250  $\text{cm}^{-1}$ ) L-Phe presented several characteristic vibrations, among which one gives a very intense band at 1004  $\text{cm}^{-1}$  arising from the phenyl ring angular bending vibrations and one at 1211  $\text{cm}^{-1}$  assigned to the side chain bond-stretching vibration  $\nu(C_\beta-C_\gamma)$ .<sup>92</sup> In the Raman spectrum of the *ex situ* prepared L-Phe-Ben2 these bands characteristic of L-Phe are clearly detectable (especially that at 1004  $\text{cm}^{-1}$ ) showing more obviously than the FT-IR spectra the deposition of the amino acid crystallites on Ben.

The spectrum of the used L-Phe-Ben2 (Fig. 10, U7) was similar to that of the hybrid before use, showing that following one reaction the material still contained a large amount of deposited L-Phe, in accordance with the XRD. In contrast, in the Raman spectrum of the material obtained *in situ* and used ten times at rt (U8) having partially lost catalytic activity, bands associated with the amino acid decreased significantly. Similarly, low intensity Raman bands were detected in the spectrum of the material obtained *in situ* after a 16 h reaction in EtOAc (U6). However, both materials still contained L-Phe, as indicated by the band at 1004  $\text{cm}^{-1}$ , though the XRD diffractogram of the latter (Fig. S14†) did not show the presence of crystalline amino acid. Accordingly, in these materials, the organic compound is distributed by adsorption on the surface and in the interlamellar space of Ben.

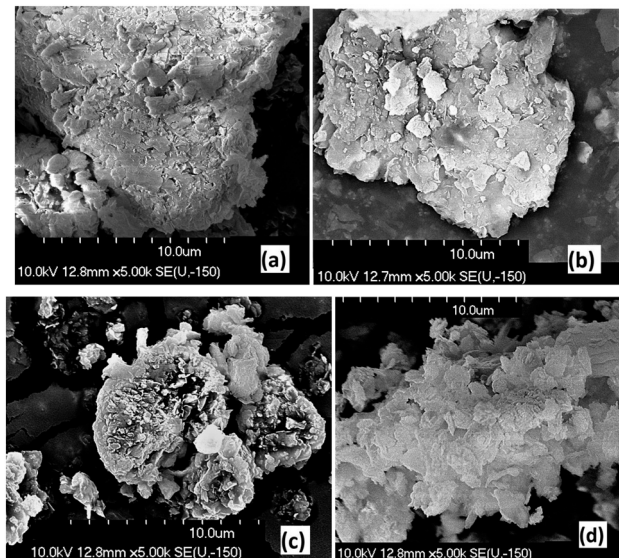


Fig. 11 SEM pictures of Ben (a), L-Phe-Ben2 (b), U1 (c) and U2 (d) (for identification of the materials see Fig. 7 and 8) at 5000 fold magnification.

Few materials employed in this study were examined by scanning electron microscopy (SEM), as these investigations proved to be useful to evidence morphological changes occurring during various treatments of montmorillonites.<sup>82–84,93</sup> Selected images are presented in Fig. 11. The parent Ben (a) showed aggregated morphology having particles bigger than 10  $\mu\text{m}$ ; however, its porous, flaky character is visible. This has not changed following *ex situ* deposition of L-Phe on Ben (L-Phe-Ben2, (b)). Smaller crystallites of irregular shapes were detected on the surface of these particles, which could be assigned to the deposited amino acid. Following the multiple uses in catalytic reactions at rt of the latter material the crystallites partially disappeared (d); moreover, the disintegration of the clay particles was also observed leading to an increase in the particle porosity. Although this decrease in the particle size could be caused by the magnetic agitation during the reaction as well, we suggest that this morphological change is partly due to the migration of the deposited amino acid into the pores and even in the interlamellar space of the layered material. This is supported by the shape of the particles obtained *in situ* in a catalytic reaction (c), which had significantly increased porosities and only slightly decreased sizes compared to Ben. The formation of such mesopores was also observed after pillaring bentonites with  $\text{Fe}^{3+}$  and  $\text{Cr}^{3+}$  cations.<sup>83</sup> Accordingly, the observed morphological change may be attributed to the presence of L-Phe in the pores and the interlamellar space of the recovered material.

### Interpretation of the results and synthetic applicability

According to the above study the asymmetric Michael addition of aldehydes to *N*-substituted maleimides is





maleimide, leading to the formation of the C–C bond. The suggested relocation of the amino acid during the reaction may occur either by dissolution and successive adsorption or by the reaction of the deposited chiral material with the aldehyde and adsorption of the enamine, as shown in Fig. 12(b).

These reactions were also catalysed efficiently by *L*-Phe immobilized over inorganic oxides lacking charge-compensating cations. Thus, the Lewis acidic sites binding the amino acid in such materials may be part of the oxide lattice as well (see  $\text{Al}_2\text{O}_3$ , ESI,† Fig. S17). The high activity of  $\text{Al}_2\text{O}_3$  may be explained by the presence of lattice defects, *i.e.* penta-coordinated Al, and the surface hydroxyl groups, characteristic of intermediate transition aluminas, such as  $\gamma\text{-Al}_2\text{O}_3$ .<sup>95,96</sup> Using layered cation-exchanger clays, the lattice cations found in the octahedral sheets may also function as binding sites of the amino acid; however, these are less accessible than the charge-compensating cations ( $\text{Na}^+$  or  $\text{Ca}^{2+}$ ), and probably their contribution is less significant.

The synthetic applicability of the developed asymmetric catalytic system was tested at a larger scale as well. Reactions

of **1a** with few *N*-substituted maleimides were carried out using 3 or 6 mmol maleimides. The products obtained are shown in Fig. 13. In these reactions a low amount of Ben (50 mg per 0.3 mmol maleimide) was used and the quantities of the reactants and EtOAc were increased proportionally. High conversions and enantioselectivities were obtained in reactions, which needed slightly prolonged times compared to those carried out at a lower scale. The solid catalysts were easily separated from the product solutions followed by isolation of the purified products in good yields by flash chromatography (eluted with hexane/EtOAc mixtures) or recrystallization in the case of crystalline crude materials (from toluene or hexane/EtOAc). Thus, the catalytic system afforded the desired optically enriched chiral compounds in gram quantities using this environmentally benign and economic catalytic system.

## Conclusions

Asymmetric Michael additions are among the most versatile C–C coupling reactions for the preparation of optically pure compounds. Green, environmentally friendly and economic catalytic systems developed for these purposes use solvents from renewable sources, natural chirality and heterogeneous, recyclable catalysts. In our present study we have investigated the asymmetric Michael addition of aldehydes to *N*-substituted maleimides catalysed by inorganic–organic hybrid materials resulting *in situ* from primary  $\alpha$ -amino acids and various inorganic oxides. Several amino acids gave efficient chiral catalysts, and the best results were obtained with the natural *L*-Phe, which afforded high conversions and excellent, up to 99% enantiomeric excesses. Various inorganic materials could be used, such as oxides or layered materials, such as cation-exchanger clays or anion-exchanger layered double hydroxides. Following optimization of the reaction conditions using two additives (bentonite and  $\text{Al}_2\text{O}_3$ ) and two solvents (diisopropyl ether and ethyl acetate), the scope of the catalytic system was extended to a large number of *N*-substituted maleimides and several aldehydes.

In the present study we have also showed that these Michael additions are catalysed by the *in situ* obtained heterogeneous chiral hybrid materials, which could be prepared *ex situ* as well and could be recycled with small activity loss. The solid material was examined by thermogravimetry, XRD, FT-IR and Raman spectroscopy, SEM and UV-vis spectroscopy-monitored adsorption experiments. Based on the results of these methods it was deduced that the amino acid is deposited as surface crystallites or intercalated in the layered cation-exchangers; however, the reactions are most probably catalysed by the chiral compounds adsorbed on the surface and the above deposits function as a supply source of the chiral organic compound compensating for the leached material. The synthetic value of the developed catalytic system was demonstrated by preparing five chiral succinimide derivatives at the gram scale. Finally, these chiral hybrid materials make it possible

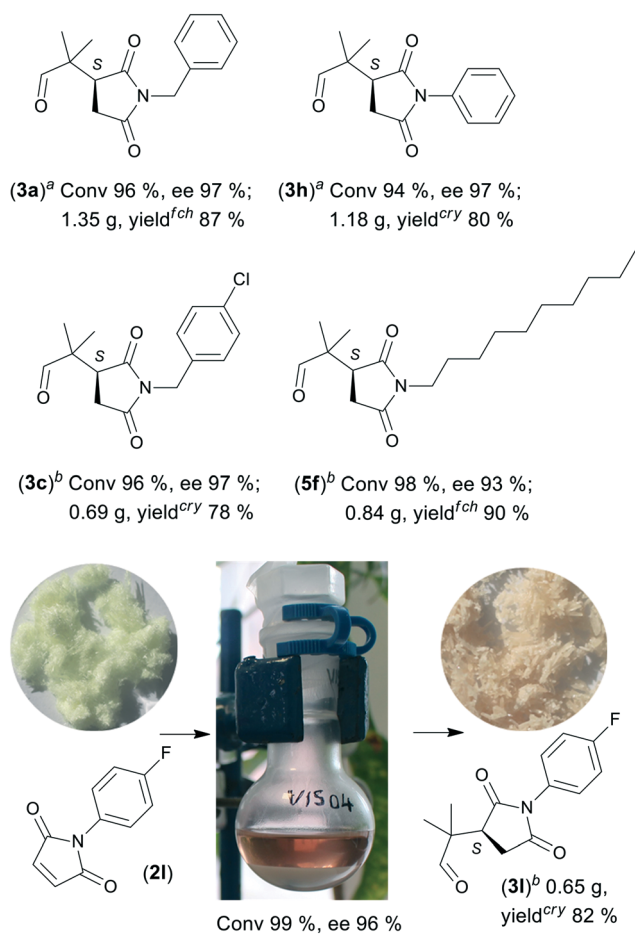


**Fig. 13** Scale-up of the Michael additions of **1a** to *N*-substituted maleimides. Reaction conditions: <sup>a</sup> 0.6 mmol *L*-Phe, 24 mmol **1a**, 6 mmol **2a** or **2h**, 1 g Ben, 20 cm<sup>3</sup> EtOAc, rt, 30 h; <sup>b</sup> 0.3 mmol *L*-Phe, 12 mmol **1a**, 3 mmol **2c**, **2l** or **4f**, 0.5 g Ben, 10 cm<sup>3</sup> EtOAc, rt, 44 h; <sup>fch</sup> isolated by flash chromatography, <sup>crv</sup> purified by recrystallization.



to obtain valuable chiral building blocks in high optical purities using a natural chirality source, a cheap inorganic solid and a non-hazardous, widely recommended organic solvent. Furthermore, these results may aid the development of other sustainable and environmentally benign procedures for the production of high-value-added optically pure fine chemicals.

## Experimental

### Materials and methods

The amino acids and their derivatives, aldehydes and ketones (**1a–1i**, Fig. S7†) and maleimides (**2a**, **2h**, **4a**, **4b**, **4k**) were commercial products (Aldrich) and used as received. The other *N*-substituted maleimides (**2b–2e**, *R-2f*, *S-2f*, **2g**, **2i–2p**, **4c–4j**, **4l**, **4m**) were prepared according to a modified literature procedure (see the ESI†).<sup>97</sup> Inorganic oxide additives: LAPONITE® RD (LAPONITE®, Lap, Southern Clay Products), bentonite H (bentonite, Ben, pH 9.5, composition: SiO<sub>2</sub> 68.1%, Al<sub>2</sub>O<sub>3</sub> 13.5%, MgO 2.9%, Fe<sub>2</sub>O<sub>3</sub> 0.7%, CaO 0.9%, Na<sub>2</sub>O 3.5%, K<sub>2</sub>O 0.1%, TiO<sub>2</sub> 0.2%, Southern Clay Products), Na-montmorillonite (Mon, Aldrich), hydrotalcite (Htc, synthetic magnesium aluminium hydroxycarbonate, Aldrich), layered double hydroxide Plural MG50 (LDH MG50, MgO/Al<sub>2</sub>O<sub>3</sub> 1/1, Sasol), Ba(OH)<sub>2</sub> (hydrate, Aldrich), Al<sub>2</sub>O<sub>3</sub> (neutral, pH 6.5–7.5, Brockman activity I, 150 mesh, 55 Å pore size, 205 m<sup>2</sup> g<sup>-1</sup> ±10% surface area, Aldrich), SiO<sub>2</sub> (high-purity grade, 35–60 mesh, Aldrich), montmorillonite K 10 (K-10, Aldrich) and Nafion™ SAC-13 (SAC-13, Aldrich) were of commercial origin. Solvents of analytical grade were used without further purification.

Products obtained in catalytic reactions were analysed by gas chromatography using an Agilent Techn. 6890 N GC-5973 MSD (GC-MSD) equipped with a 30 m long DB-1MS UI (J&W, Agilent) capillary column for mass spectrometric identification of the compounds and an Agilent 7890A GC-FID (GC-FID) equipped with chiral capillary columns (Cyclosil-B, 30 m × 0.25 mm, J&W, Agilent; HP-Chiral-20B, 30 m × 0.25 mm, J&W, Agilent or Hydrodex g-TBDAC, 25 m × 0.25 mm, Macherey-Nagel) for quantitative analysis. <sup>1</sup>H- and <sup>13</sup>C-NMR spectra were recorded on a Bruker DRX-500 spectrometer at 500 (<sup>1</sup>H) and 125 (<sup>13</sup>C) MHz in CDCl<sub>3</sub> solvent using tetramethylsilane as an internal standard.

Adsorption experiments were followed by UV-vis spectroscopy on a Jenway 6850 UV/vis double beam spectrophotometer with 0.1 nm wavelength resolution using a deuterium lamp and 10 mm path length quartz cuvettes. Thermal analysis (thermogravimetry, TG and differential thermogravimetry, DTG) of the materials was carried out in air at a 10 °C min<sup>-1</sup> heating rate using a Setaram Labsys instrument and ≈30 mg samples. X-ray diffractograms (XRD) were recorded on a Rigaku Miniflex-II diffractometer using Cu K $\alpha$  radiation ( $\lambda$  = 0.1548 nm) at a scanning rate of 4° min<sup>-1</sup> between 2 and 30° 2 $\theta$  angles. FT-IR measurements were recorded on a Bio-Rad Digilab Divison FTS-65A/896

spectrometer operating in diffuse reflectance mode between 4000 and 400 cm<sup>-1</sup> using 2 cm<sup>-1</sup> resolution by averaging 256 scans. 0.02 g samples were mixed with 0.18 g powdered dry KBr. Raman spectra were recorded with a confocal Bruker Senterra II Raman microscope. A 785 nm laser for excitation and 100 mW laser power were applied. An average of 16 scans with 4 cm<sup>-1</sup> spectral resolution and an exposition time of 6 s in the 400–4000 cm<sup>-1</sup> spectral range were recorded. Scanning electron microscopy (SEM) measurements using 10 kV accelerating voltage were carried out on a Hitachi S-4700 Type II FE-SEM instrument. Samples mounted on conductive carbon tape were sputter coated with a thin Au/Pd layer prior to measurements.

### Ex situ preparation of chiral hybrid materials

These materials were prepared by stirring magnetically (800 rpm) in a 25 cm<sup>3</sup> round-bottom flask a slurry containing 500 mg Ben and 0.3 mmol *L*-Phe in 10 cm<sup>3</sup> EtOAc (*L*-Phe–Ben1) or <sup>1</sup>Pr<sub>2</sub>O (*L*-Phe–Ben2) for 6 h. The solid material was centrifuged and washed twice with 10 cm<sup>3</sup> of the corresponding solvent. Following drying under ambient conditions to constant weight the materials were stored in vials until use. The hybrid materials using 0.3 mmol **1a**, **2a** or *S-3a* were prepared similarly.

### Michael additions: general procedure

In a typical run, the given amount of inorganic additive and 0.03 mmol amino acid were suspended in 1 cm<sup>3</sup> solvent (typically in EtOAc or <sup>1</sup>Pr<sub>2</sub>O) in a 4 cm<sup>3</sup> closed glass vial by magnetic stirring. Following addition of 0.3 mmol *N*-substituted maleimide and 1.2 mmol carbonyl compound the reaction was carried out by stirring the slurry (800 rpm) for the given time. During reactions at higher than room temperatures, the vials were immersed in a preheated oil bath. Following the desired reaction time the mixture was diluted with 2 cm<sup>3</sup> solvent and centrifuged. The solid material was washed twice with 2 cm<sup>3</sup> solvent, and the resulting solid material was dried under ambient conditions and further used in recycling or characterization experiments. The unified supernatants were analysed by GC-MSD and GC-FID following addition of *n*-decane internal standard. Conversion (Conv) and enantiomeric excess (ee) were calculated using the results of the latter analysis and formulae given in the ESI.† The absolute configuration of the excess enantiomer was assigned based on previous reports.<sup>36,38,39,43,59,62</sup> The crude product was obtained by evaporating the solvent and the unreacted aldehyde (if possible) and was purified by flash chromatography using hexane/EtOAc or hexane/<sup>t</sup>BuOMe (see the ESI†) or in the case of solid raw products by recrystallization from toluene or hexane/EtOAc to determine the yield. The pure product was further analysed by GC-FID, <sup>1</sup>H- and <sup>13</sup>C-NMR. The NMR spectra of the purified products were identical with the spectra published in the literature. Reactions at a larger scale (3 or 6 mmol maleimides) were carried out similarly



in a single-neck round-bottom flask of 25 or 50 cm<sup>3</sup> by increasing proportionally the quantities of the reaction components.

## Author contributions

The authors contributed equally to the research work.

## Conflicts of interest

There are no conflicts to declare.

## Acknowledgements

Financial support by the Hungarian Ministry of Human Capacities through grant 20391-3/2018/FEKUSTRAT is highly appreciated. Financial support of the Hungarian Science Foundation through OTKA Grant K 138871 is acknowledged. The authors thank Dr. Gábor Varga, Dr. Márton Szabados, Dr. Rebeka Mészáros, Prof. Ákos Kukovecz and Prof. Zoltán Kónya for their valuable help in characterizing the hybrid materials.

## References

- 1 *Handbook of Chiral Chemicals*, ed. D. Ager, CRC Press, Taylor & Francis Group, Boca Raton, 2nd edn, 2006.
- 2 *Common Fragrance and Flavor Materials, Preparation, Properties and Uses*, ed. H. Surburg and J. Panten, Wiley-VCH, Verlag GmbH, Weinheim, 6th edn, 2016.
- 3 *Chiral Drugs, Chemistry and Biological Action*, ed. G.-Q. Lin, Q.-D. You and J.-F. Cheng, John Wiley & Sons, Inc., Hoboken, New Jersey, 2011.
- 4 V. Šunjić and M. J. Parnham, *Signposts to Chiral Drugs, Organic Synthesis in Action*, Springer Basel AG, Basel, 2011.
- 5 *Asymmetric Catalysis on Industrial Scale, Challenges, Approaches and Solutions*, ed. H. U. Blaser and E. Schmidt, Wiley-VCH, Verlag GmbH, Weinheim, 2004.
- 6 *Catalytic Asymmetric Synthesis*, ed. I. Ojima, John Wiley & Sons, Inc., Hoboken, New Jersey, 3rd edn, 2010.
- 7 *Catalytic Methods in Asymmetric Synthesis, Advanced Materials, Techniques, and Applications*, ed. M. Gruttadauria and F. Giacalone, John Wiley & Sons, Inc., Hoboken, New Jersey, 2011.
- 8 H. Pellissier, *Recent Developments in Asymmetric Organocatalysis*, RSC Catalysis Series No. 3, RSC Publ., Cambridge, 2010.
- 9 *Science of Synthesis: Asymmetric Organocatalysis 1, Lewis Base and Acid Catalysts*, ed. B. List, Thieme, Stuttgart, 2012.
- 10 *Science of Synthesis: Asymmetric Organocatalysis 2, Brønsted Base and Acid Catalysts, and Additional Topics*, ed. K. Maruoka, Thieme, Stuttgart, 2012.
- 11 *Comprehensive Enantioselective Organocatalysis, Catalysts, Reactions, and Applications*, ed. P. I. Dalko, Wiley-VCH, Verlag GmbH, Weinheim, 2013.
- 12 *Catalytic Asymmetric Conjugate Reactions*, ed. A. Córdova, Wiley-VCH, Verlag GmbH, Weinheim, 2010.
- 13 *Organocatalytic Enantioselective Conjugate Addition Reactions, A Powerful Tool for the Stereocontrolled Synthesis of Complex Molecules*, RSC Catalysis Series No. 5, ed. J. L. Vicario, D. Badía, L. Carrillo and E. Reyes, RSC Publ., Cambridge, 2010.
- 14 M. L. Curtin, R. B. Garland, H. R. Heyman, R. R. Frey, M. R. Michaelides, J. Li, L. J. Pease, K. B. Glaser, P. A. Marcotte and S. K. Davidsen, *Bioorg. Med. Chem. Lett.*, 2002, **12**, 2919–2923.
- 15 J. Uddin, K. Ueda, E. R. O. Siwu, M. Kita and D. Uemura, *Bioorg. Med. Chem.*, 2006, **14**, 6954–6961.
- 16 S. Ahmad, M. H. Mahnashi, B. A. Alyami, Y. S. Alqahtani, F. Ullah, M. Ayaz, M. Tariq, A. Sadiq and U. Rashid, *Drug Des., Dev. Ther.*, 2021, **15**, 1299–1313.
- 17 P. Chauhan, J. Kaur and S. S. Chimni, *Chem. – Asian J.*, 2013, **8**, 328–346.
- 18 G. Bartoli, M. Bosco, A. Carlone, A. Cavalli, M. Locatelli, A. Mazzanti, P. Ricci, L. Sambri and P. Melchiorre, *Angew. Chem., Int. Ed.*, 2006, **45**, 4966–4970.
- 19 X. Huang, W.-B. Yi, D. Ahad and W. Zhang, *Tetrahedron Lett.*, 2013, **54**, 6064–6066.
- 20 S. Mahajan, P. Chauhan, A. Kumar and S. S. Chimni, *Tetrahedron: Asymmetry*, 2016, **27**, 1145–1152.
- 21 N. Di Iorio, F. Champavert, A. Erice, P. Righi, A. Mazzanti and G. Bencivenni, *Tetrahedron*, 2016, **72**, 5191–5201.
- 22 G.-L. Zhao, Y. Xu, H. Sundén, L. Eriksson, M. Sayah and A. Córdova, *Chem. Commun.*, 2007, 734–735.
- 23 J. Wang, M.-M. Zhang, S. Zhang, Z.-A. Xu, H. Li, X.-H. Yu and W. Wang, *Synlett*, 2011, 473–476.
- 24 F. Yu, X. Sun, Z. Jin, S. Wen, X. Liang and J. Ye, *Chem. Commun.*, 2010, **46**, 4589–4591.
- 25 F. Yu, Z. Jin, H. Huang, T. Ye, X. Liang and J. Ye, *Org. Biomol. Chem.*, 2010, **8**, 4767–4774.
- 26 F. Xue, L. Liu, S. Zhang, W. Duan and W. Wang, *Chem. – Eur. J.*, 2010, **16**, 7979–7982.
- 27 J.-F. Bai, L. Peng, L.-L. Wang, L. X. Wang and X.-Y. Xu, *Tetrahedron*, 2010, **66**, 8928–8932.
- 28 Z. Ma, Y. Liu, P. Li, H. Ren, Y. Zhu and J. Tao, *Tetrahedron: Asymmetry*, 2011, **22**, 1740–1748.
- 29 T. Miura, S. Nishida, A. Masuda, N. Tada and A. Itoh, *Tetrahedron Lett.*, 2011, **52**, 4158–4160.
- 30 E. Gómez-Torres, D. A. Alonso, E. Gómez-Bengoia and C. Nájera, *Org. Lett.*, 2011, **13**, 6106–6109.
- 31 A. Avila, R. Chinchilla and C. Nájera, *Tetrahedron: Asymmetry*, 2012, **23**, 1625–1627.
- 32 J. Flores-Ferrándiz and R. Chinchilla, *Tetrahedron: Asymmetry*, 2014, **25**, 1091–1094.
- 33 K. Nakashima, M. Kawada, S. Hirashima, M. Kato, Y. Koseki and T. Miura, *Synlett*, 2015, **26**, 1248–1252.
- 34 P. Vizcaíno-Milla, J. M. Sansano, C. Nájera, B. Fiser and E. Gómez-Bengoia, *Synthesis*, 2015, **47**, 2199–2206.
- 35 A. Torregrosa-Chinillach, A. Moragues, H. Pérez-Furundarena, R. Chinchilla, E. Gómez-Bengoia and G. Guillena, *Molecules*, 2018, **23**, 3299.
- 36 V. Kozma, F. Fülöp and G. Szöllösi, *Adv. Synth. Catal.*, 2020, **362**, 2444–2458.
- 37 V. Kozma and G. Szöllösi, *Mol. Catal.*, 2022, **518**, 112089.



- 38 T. C. Nugent, A. Sadiq, A. Bibi, T. Heine, L. L. Zeonjuk, N. Vankova and B. S. Bassil, *Chem. – Eur. J.*, 2012, **18**, 4088–4098.
- 39 C. G. Kokotos, *Org. Lett.*, 2013, **15**, 2406–2409.
- 40 S. Muramulla, J.-A. Ma and J. C.-G. Zhao, *Adv. Synth. Catal.*, 2013, **355**, 1260–1264.
- 41 C. E. Grünenfelder, J. K. Kisunzu and H. Wennemers, *Angew. Chem., Int. Ed.*, 2016, **55**, 8571–8574.
- 42 A. Schiza, N. Spiliopoulou, A. Shahu and C. G. Kokotos, *New J. Chem.*, 2018, **42**, 18844–18849.
- 43 A. Sadiq and T. C. Nugent, *ChemistrySelect*, 2020, **5**, 11934–11938.
- 44 W. Ye, Z. Jiang, Y. Zhao, S. L. M. Goh, D. Leow, Y.-T. Soh and C.-H. Tan, *Adv. Synth. Catal.*, 2007, **349**, 2454–2458.
- 45 Z. Jiang, Y. Pan, Y. Zhao, T. Ma, R. Lee, Y. Yang, K.-W. Huang, M. W. Wong and C.-H. Tan, *Angew. Chem., Int. Ed.*, 2009, **48**, 3627–3631.
- 46 V. J. Kolcsár and Gy. Szöllösi, *Catal. Sci. Technol.*, 2021, **11**, 7652–7666.
- 47 *Chiral Catalyst Immobilization and Recycling*, ed. D. E. De Vos, I. F. J. Vankelecom and P. A. Jacobs, Wiley-VCH, Verlag GmbH, Weinheim, 2000.
- 48 *Handbook of Asymmetric Heterogeneous Catalysis*, ed. K. Ding and Y. Uozumi, Wiley-VCH, Verlag GmbH, Weinheim, 2008.
- 49 *Enantioselective Homogeneous Supported Catalysis*, RSC Green Chemistry Series No. 15, ed. R. Šebesta, RSC Publ., Cambridge, 2012.
- 50 *Catalyst Immobilization, Methods and Applications*, ed. M. Benaglia and A. Puglisi, Wiley-VCH, Verlag GmbH, Weinheim, 2020.
- 51 Gy. Szöllösi, *Catal. Sci. Technol.*, 2018, **8**, 389–422.
- 52 Y. Qin, G. Yang, L. Yang, J. Li and Y. Cui, *Catal. Lett.*, 2011, **141**, 481–488.
- 53 L. Yang, D. Zhou, C. Qu and Y. Cui, *Catal. Lett.*, 2012, **142**, 1405–1410.
- 54 Y. Qin, W. Zhao, L. Yang, X. Zhang and Y. Cui, *Chirality*, 2012, **24**, 640–645.
- 55 W. Zhao, Y. Zhang, C. Qu, L. Zhang, J. Wang and Y. Cui, *Catal. Lett.*, 2014, **144**, 1681–1688.
- 56 S. H. Newland, D. J. Xuereb, E. Gianotti, L. Marchese, R. Rios and R. Raja, *Catal. Sci. Technol.*, 2015, **5**, 660–665.
- 57 H. Zhang, W. Yang and J. Deng, *Polymer*, 2015, **80**, 115–122.
- 58 S. V. Kochetkov, A. S. Kucherenko and S. G. Zlotin, *Mendeleev Commun.*, 2017, **27**, 473–475.
- 59 Gy. Szöllösi and V. Kozma, *ChemCatChem*, 2018, **10**, 4362–4368.
- 60 S.-X. Cao, J.-X. Wang and Z.-J. He, *Chin. Chem. Lett.*, 2018, **29**, 201–204.
- 61 H. Zhang, Q. Zhang, C. Hong and G. Zou, *Polym. Chem.*, 2017, **8**, 1771–1777.
- 62 J. M. Landeros, C. Cruz-Hernández and E. Juaristi, *Eur. J. Org. Chem.*, 2021, 5117–5126.
- 63 B. M. Choudary, M. L. Kantam, K. V. S. Ranganath, K. Mahendar and B. Sreedhar, *J. Am. Chem. Soc.*, 2004, **126**, 3396–3397.
- 64 B. M. Choudary, K. V. S. Ranganath, U. Pal, M. L. Kantam and B. Sreedhar, *J. Am. Chem. Soc.*, 2005, **127**, 13167–13171.
- 65 B. M. Choudary, L. Chakrapani, T. Ramani, K. V. Kumar and M. L. Kantam, *Tetrahedron*, 2006, **62**, 9571–9576.
- 66 L. Zhong, J. Xiao and C. Li, *J. Catal.*, 2006, **243**, 442–445.
- 67 S. Vijaikumar, A. Dhakshinamoorthy and K. Pitchumani, *Appl. Catal., A*, 2008, **340**, 25–32.
- 68 G. Szöllösi, M. Fekete, A. A. Gurka and M. Bartók, *Catal. Lett.*, 2014, **144**, 478–486.
- 69 K. Szőri, B. Réti, G. Szöllösi, K. Hernádi and M. Bartók, *Top. Catal.*, 2016, **59**, 1227–1236.
- 70 Gy. Szöllösi, D. Gombkötő, A. Zs. Mogyorós and F. Fülöp, *Adv. Synth. Catal.*, 2018, **360**, 1992–2004.
- 71 X.-B. Huang, J.-S. Sun, Y. Huang, B.-C. Yan, X.-D. Dong, F. Liu and R. Wang, *Pet. Sci.*, 2021, **18**, 579–590.
- 72 F. P. Byrne, S. Jin, G. Paggiola, T. H. M. Petchey, J. H. Clark, T. J. Farmer, A. J. Hunt, R. McElroy and J. Sherwood, *Sustainable Chem. Processes*, 2016, **4**, 7.
- 73 A. Meunier, *Clays*, Springer-Verlag, Berlin, Germany, 2005.
- 74 *Handbook of Clay Science*, ed. F. Bergaya, B. K. G. Theng and G. Lagaly, Elsevier, Oxford, UK, 1st edn, 2006.
- 75 K. R. Reddy, A. El-Zein, D. W. Airey, F. Alonso-Marroquin, P. Schubel and A. Manalo, *Nano-Struct. Nano-Objects*, 2020, **23**, 100500.
- 76 H. Bayram, M. Önal, H. Yilmaz and Y. Sarikaya, *J. Therm. Anal. Calorim.*, 2010, **101**, 873–879.
- 77 S. Zymankowska-Kumon, M. Holtzer and G. Grabowski, *Arch. Foundry Eng.*, 2011, **11**, 209–213.
- 78 M. V. Kok, *Energy Sources, Part A*, 2014, **36**, 173–183.
- 79 Á. Fudala, I. Pálinkó and I. Kiricsi, *Inorg. Chem.*, 1999, **38**, 4653–4658.
- 80 R. D. Gougeon, M. Soulard, J. Miché-Brendlé, J.-M. Chézeau, R. Le Dred, P. Jeandet and R. Marchal, *J. Agric. Food Chem.*, 2003, **51**, 4096–4100.
- 81 H. Sun, T. Peng, B. Liu and H. Xian, *Appl. Clay Sci.*, 2015, **114**, 440–446.
- 82 Y. Qin, T. Peng, H. Sun, L. Zeng and C. Zhou, *Clays Clay Miner.*, 2021, **69**, 328–338.
- 83 F. Tomul, *Ind. Eng. Chem. Res.*, 2011, **50**, 7228–7240.
- 84 S. Mallakpour and M. Dinari, *Appl. Clay Sci.*, 2011, **51**, 353–359.
- 85 S. Mallakpour and A. Barati, *Polym.-Plast. Technol. Eng.*, 2012, **51**, 321–327.
- 86 M. S. Yilmaz, Y. Kalpakli and S. Pişkin, *J. Therm. Anal. Calorim.*, 2013, **114**, 1191–1199.
- 87 N. R. Smart, B. Reddy, A. P. Rance, D. J. Nixon and N. Diomidis, *Corros. Eng., Sci. Technol.*, 2017, **52**, 113–126.
- 88 E. Steger, A. Turcu and V. Macovei, *Spectrochim. Acta*, 1963, **19**, 293–300.
- 89 H.-Q. Li, A. Chen, S. G. Roscoe and J. Lipkowski, *J. Electroanal. Chem.*, 2001, **500**, 299–310.
- 90 R. L. Frost and L. Rintoul, *Appl. Clay Sci.*, 1996, **11**, 171–183.
- 91 J. L. Bishop and E. Murad, *J. Raman Spectrosc.*, 2004, **35**, 480–486.



- 92 B. Hernández, F. Pflüger, S. G. Kruglik and M. Ghomi, *J. Raman Spectrosc.*, 2013, **44**, 827–833.
- 93 S. T. Ferrazzo, R. de Souza Tímbola, L. Bragagnolo, E. Prestes, E. P. Korf, P. D. M. Prietto and C. Ulsen, *Environ. Sci. Pollut. Res.*, 2020, **27**, 37718–37732.
- 94 L. Chen and S. Luo, in: *Enantioselective Organocatalyzed Reactions I: Enantioselective Oxidation, Reduction, Functionalization and Desymmetrization*, ed. R. Mahrwald, Springer Sci., Dordrecht, 2011, ch. 5, pp. 147–184.
- 95 C. V. Chandran, C. E. A. Kirschhock, S. Radhakrishnan, F. Taulelle, J. A. Martens and E. Breynaert, *Chem. Soc. Rev.*, 2019, **48**, 134–156.
- 96 R. Prins, *J. Catal.*, 2020, **392**, 336–346.
- 97 S. Firoozi, M. Hosseini-Sarvari and M. Koohgard, *Green Chem.*, 2018, **20**, 5540–5549.

